LAPPEENRANTA UNIVERSITY OF TECHNOLOGY
Faculty of Technology
LUT Chemistry

Salla Hiltunen

MODELING STUDY OF LIMESTONE REACTIONS IN FLUIDIZED BED CONDITIONS

Examiners Professor Heli Sirén
Professor Timo Hyppänen

Instructor D.Sc. (Tech.) Tero Tynjälä

ABSTRACT

Lappeenranta University of Technology
Faculty of Technology
LUT Chemistry

Salla Hiltunen

Modeling study of limestone reactions in fluidized bed conditions

Master's Thesis

2011

58 pages, 26 figures, 2 tables

Examiners Professor Heli Sirén
Professor Timo Hyppänen

Keywords: calcium looping cycle, O_2/CO_2 combustion, calcination, sulfation, carbonation

Traditionally limestone has been used for the flue gas desulfurization in fluidized bed combustion. Recently, several studies have been carried out to examine the use of limestone in applications which enable the removal of carbon dioxide from the combustion gases, such as calcium looping technology and oxy-fuel combustion. In these processes interlinked limestone reactions occur but the reaction mechanisms and kinetics are not yet fully understood. To examine these phenomena, analytical and numerical models have been created.

In this work, the limestone reactions were studied with aid of one-dimensional numerical particle model. The model describes a single limestone particle in the process as a function of time, the progress of the reactions and the mass and energy transfer in the particle. The model-based results were compared with experimental laboratory scale BFB results.

It was observed that by increasing the temperature from 850 °C to 950 °C the calcination was enhanced but the sulfate conversion was no more improved. A higher sulfur dioxide concentration accelerated the sulfation reaction and based on the modeling, the sulfation is first order with respect to SO_2. The reaction order of O_2 seems to become zero at high oxygen concentrations.

TIIVISTELMÄ

Lappeenrannan teknillinen yliopisto
Teknillinen tiedekunta
LUT Kemia

Salla Hiltunen

Mallipohjainen tarkastelu kalkkikiven reaktioista leijukattiloissa

Diplomityö

2011

58 sivua, 26 kuvaa, 2 taulukkoa

Tarkastajat Professori Heli Sirén
Professori Timo Hyppänen

Hakusanat: kalsiumkiertoprosessi, happipoltto, kalsinointi, sulfatointi, karbonointi

Kalkkikiveä on perinteisesti käytetty leijukattiloissa rikinsidontaan. Viimeaikoina on tutkittu intensiivisesti kalkkikiven käyttöä myös hiilidioksidin poiston mahdollistavissa sovelluksissa, kuten kalsiumkiertoprosessissa ja happipoltossa. Molemmissa prosesseissa kalkkikivi voi reagoida useilla toisiinsa kytkeytyneillä reaktioilla, joiden mekanismia ja kinetiikkaa ei ole vielä täysin ymmärretty. Ilmiöiden tutkimiseksi on kehitetty sekä analyyttisiä että numeerisia malleja.

Tässä työssä tutkittiin kalkkikiven reaktioita käyttämällä apuna yksiulotteista numeerista partikkelimallia. Malli kuvaa systeemissä olevaa yksittäistä kalkkipartikkelia ajan funktiona ja partikkelin sisällä tapahtuvaa aineen- ja energiansiirtoa. Mallin laskentatuloksia verrattiin kokeellisiin, laboratoriomittakaavan BFB -kattilalla saatuihin mittaustuloksiin.

Työssä havaittiin, että lämpötilan kasvattaminen 850 °C:sta 950 °C:een edisti erityisesti kalsinoitumisreaktiota, mutta ei enää parantanut sulfatoitumisastetta. Suurempi rikkidioksidipitoisuus kasvatti sulfatoitumisnopeutta ja mallinnuksen perusteella rikin kertaluku sulfatoitumisreaktiossa on yksi. Suurissa happipitoisuuksissa hapen määrällä ei näyttäisi olevan vaikutusta sulfatointireaktioon.

CONTENTS

LIST OF SYMBOLS

Roman Symbols

A	area [m^2]
C	concentration [mol/m^3]
c_p	heat capacity in constant pressure [J/kgK]
d	diameter [m]
D	diffusion coefficient [m^2/s]
E_a	activation energy [J/mol]
h	enthalpy [J/kg]
k	thermal conductivity [W/mK], rate constant [mol/m^2s]
M	molar mass [kg/mol]
P	pressure [Pa]
R	radius of the particle [m]
r	reaction rate, radial coordinate within the particle [m]
Re	Reynold's number [-]
S	specific surface area [m^2/m^3], source term
Sh	Sherwood number [-]
T	temperature [K]
t	time [s]
v	velocity [m/s]
V	volume [m^3]
W	weight percentage
X	conversion [-]

Greek symbols

ε	volume fraction [-]
v	stoichiometric coefficient [-]
ρ	density [kg/m^3]
Φ	Thiele modulus [-]

Subscripts

eff	effective
eq	equilibrium
g	gas
i	species i
s	solid
tot	total

Abbreviations

AFBC	atmospheric fluidized bed combustion
BFB	bubbling fluidized bed
CCS	carbon capture and storage
SEM-EDS	scanning electron microscope–energy-dispersive spectrometry

1 INTRODUCTION

Calcium looping and oxy-fuel combustion are techniques which are intensively studied at the moment in order to control the CO_2 emissions of power plants. In these combustion techniques the conditions in the boiler differ from normal air-fired units. For this purpose, models that can predict the effects of the changed environment on the burning process are needed. The development of the large industrial scale models requires profound understanding of particle scale phenomena. In this study, different methods (bench scale tests, numerical modeling and SEM-EDS analysis) were used to study the limestone reactions. The theoretical part discusses the phenomena especially from calcium-looping process point of view.

In the calcium looping cycle, the removal of CO_2 from the combustion gases is done in two stages. In the first unit, CO_2 is captured from flue gases with aid of calcium oxide. In the second unit, the CO_2 is then released thermally from the sorbent and the concentrated stream of CO_2 is purified, liquefied and stored. The CaO is recycled back to the first stage. The application is planned to carry out in two connected fluidized bed reactors.

The advantage of calcium-looping cycle is that it has relatively small effects to the efficiency of a power plant (reduction of 6-8%) when compared to other technologies such as amine scrubbing (Blamey *et al*. 2010). Limestone is a cheap sorbent, commonly available and its handling is rather easy. The oxy-fuel combustion enables high concentrations of CO_2 and the flue gas stream is almost nitrogen free. It has been estimated that approximately 80-90% CO_2 removal could be achieved with this technique (Anthony 2011).

One of the main problems of the looping cycles is that limestone loses its capture capacity when it is constantly circulated between the two reactors. This is due to competing sulfation reactions which are irreversible in the process conditions. Attrition and sintering also weaken the sorbent capture capacity. In addition to process technical challenges, the disposal of captured CO_2 is under discussion. Part of the CO_2 could possibly be used in other industrial applications (e.g. industrial production of urea, enhanced oil recovery, production of synthetic plastics), but still huge amounts of captured CO_2 would remain unexploited. Current solution is to store the CO_2 into

geological formations, such as depleted oil fields or saline aquifers. In these cases the escape of the gas has to be prevented.

At the moment, pilot plant testing of the calcium looping technology is ongoing and the technology is part of European Union CCS plan.

2 CHEMICAL REACTIONS IN CALCIUM LOOPING CYCLES

The calcium looping cycle is carried out at high temperature and in an atmosphere containing carbon dioxide, water vapor and sulphur dioxide. These conditions set a severe environment where interlinked reactions, i.e. calcination, carbonation, sulfation and desulfation take place. Due to the high temperature and mechanical stress, also fragmentation and sintering of the limestone occur. (Stanmore and Gilot 2005)

The principle of the calcium-looping cycle for post-combustion CO_2 capture is shown in figure 1. It consists of dual-fluidized bed system, calciner and carbonator. The fresh limestone is first fed to the calciner where it starts its cyclic movement in the process. The temperature level in the calciner is 850–950 °C and in the carbonator 600–700 °C.

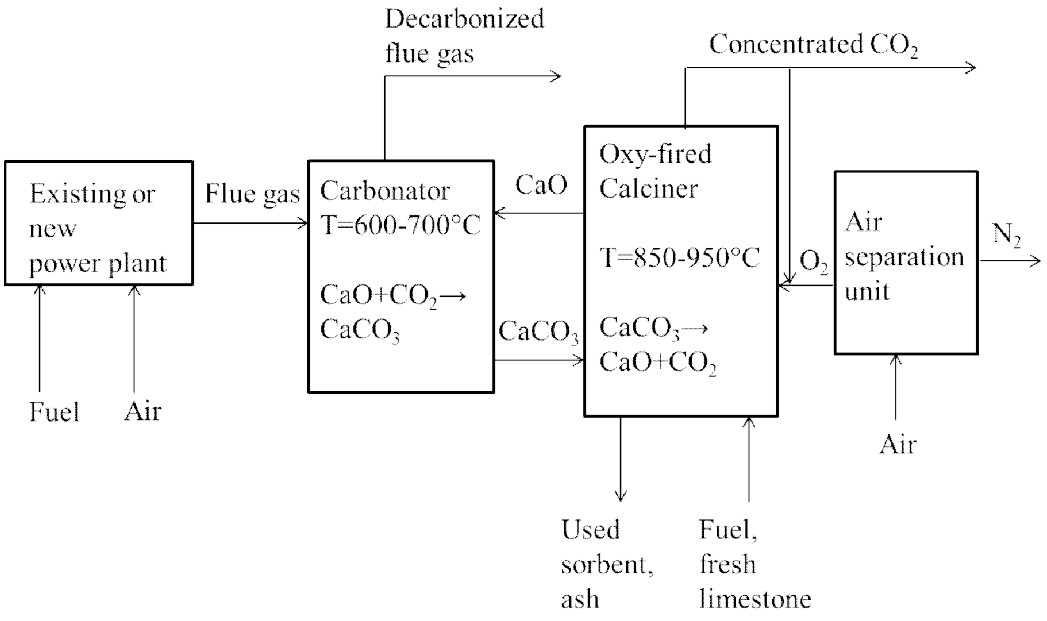

Figure 1 Calcium-looping cycle for post-combustion CO_2 capture. Modified from Sánchez-Biezma *et al.* (2011).

2.1 Calcination

All the fresh limestone fed to the system has to first pass through the calcination step before it can be used for CO_2 capture, as well as the used sorbent is regenerated in the calciner according to the reaction (1):

$$CaCO_3(s) \rightleftarrows CaO(s) + CO_2(g). \quad (1)$$

The reaction can be described to occur in four stages: it starts with the thermal decomposition of $CaCO_3$ and is followed by the diffusion of CO_2 trough the internal voids of the particle. In the third phase the CO_2 diffuses from the particle surface to the bulk gas. The particle is continuously formed during the process: the calcination reaction changes the particle structure from slightly porous ($\varepsilon = 0.03–0.3$) to very porous solid material ($\varepsilon > 50$) which has a high surface area. As the reaction proceeds, the surface area and porosity are decreasing due to high temperature and sintering. (Silcox *et al*. 1989)

The calcination can be controlled by chemical reaction, mass transfer or heat transfer. (Silcox *et al*. 1989, Stanmore and Gilot 2005). The reactivity of limestone depends on the cycle number, gas components (e.g. contents of CO_2, SO_2 and water vapor), temperature, particle size, impurities and the composition and morphology of the limestone particle. The main goal is to understand the effect of each parameter on the reaction.

2.1.1 Diffusion

In the thermal decomposition of limestone, CO_2 is discharged. In the particle, the CO_2 cannot diffuse freely because the flow is affected by the collisions with pore walls and with the other CO_2 molecules. Thus the mass transfer of CO_2 may become rate limiting, especially when the calcination reaction itself is fast. A mathematical description of the CO_2 diffusion in the pores is very complex, since the pores form a connected network inside the particle and the pore sizes as well as their shape alter continuously.

In the literature, the diffusion of CO_2 in the porous lime is typically described with Knudsen diffusion, molecular diffusion, pore diffusion and effective diffusion. The Knudsen diffusion occurs in the very narrow pores (small pore diameter), where the diffusion is limited by collisions with the pore walls. For the larger pores, molecular diffusion, where flow depends on the intermolecular collisions, is used. These two flows, Knudsen diffusion and molecular diffusion, are then combined together to describe the CO_2 flow in the porous particle, forming so called pore diffusion. However,

since the particle porosity is changing continuously with the calcination reaction, it has to be considered. Thus, effective diffusion is introduced: it is an average estimate for the total diffusion coefficient in the particle and is a function of the particle porosity. In addition, the effective diffusivity depends on the gas composition, temperature and pressure. Both Silcox *et al*. (1989) and García-Labiano *et al*. (2002) used above-mentioned technique to determine the effective diffusion coefficient for CO_2 in the porous limestone, but ended up with very different results. In the study of Silcox *et al*. (1989), the pore diffusion coefficient was approximately $1.7 \cdot 10^{-3}$ m^2/s at 850 °C whereas in the work of García-Labiano *et al*. (2002) the pore diffusion coefficient at 850 °C was about $2.2 \cdot 10^{-5}$ m^2/s. Especially the Knudsen diffusion is strongly dependent on the pore geometry which may cause remarkable differences when evaluating the diffusion coefficient (Levitz 1993). According to Cussler (1997), the measured diffusion coefficient for air-CO_2 gas pair is approximately $1.77 \cdot 10^{-5}$ m^2/s at 44 °C and at one atmosphere, but the value depends on temperature: as temperature is increased the diffusion coefficient increases as well.

2.1.2 Reaction kinetics

In the literature, several correlations for the calcination reaction exist. Since the reaction is a heterogenic gas-solid reaction, many researchers have used a model in which the reaction rate depends on the surface area of the reacting solid. Hu and Scaroni (1996) suggested the following expression for the calcination reaction:

$$r = -k(T) \cdot A_{CaCO_3} \cdot f(P_{CO_2}) \qquad (2)$$

in which

r	reaction rate for calcination [mol/s]
k	reaction rate coefficient, a function of temperature [mol/m^2s]
A_{CaCO_3}	surface area (BET) of the reacting solid [m^2]
$f(P_{CO2})$	function of CO_2 partial pressure.

Later, García-Labiano *et al*. (2002) used a similar expression in their modeling study. The weakness of these correlations is the dependence of the surface area. The surface area is difficult to estimate reliably, it varies between the different limestone types and

is continuously alternating during the reaction. A wrong estimate causes mistakes in the calculation. In the modeling, the surface area in which the reactions take place (effective surface area) should be used. (Hu *et al*. 2006)

Recently, Takkinen *et al*. (2011) used a model (eq. 3), in which the reaction rate was no more dependent on the surface area but instead on the mass fraction of the reacting solid:

$$r = k \cdot f(T) \cdot f\left(P_{CO_2}\right) \cdot f(Y_{CaCO3}), \quad (3)$$

in which

r reaction rate for calcination [mol/m^{3}s]
Y_{CaCO_3} mass fraction of $CaCO_3$ [-].

2.1.3 Effect of temperature

Temperature has significant effect on calcination. Since the reaction is endothermic, high temperature is required so that sufficient calcination conversion is achieved in reasonable time. Extensive increase of temperature is not, however, advisable since sintering is enhanced at high temperatures. Sintering causes surface area losses and reduces the porosity of the particle.

Typically, an Arrhenius type equation is used to describe the temperature dependence of the of the reaction rate coefficient:

$$k = Ae^{\frac{-E_a}{RT}}, \quad (4)$$

where

A frequency factor
E_a activation energy
R universal gas constant
T temperature.

Silcox *et al*. (1989) used an equation (5) for the reaction rate coefficient

$$k = 1.22e^{\frac{-4026}{T}}. \quad (5)$$

Rao (1996) defined for temperature range 737-875 °C the following equation (6)

$$k = 16.68e^{\frac{-1.18\cdot10^8}{RT}}. \quad (6)$$

Hu and Scaroni (1996) used the equation (7) for the temperature dependence of the reaction rate coefficient

$$k = 6.078 \cdot 10^7 e^{\frac{-205000}{RT}}. \quad (7)$$

As it can be observed, the values obtained for the reaction rate coefficients and for the activation energy differ remarkably between the research groups. Ray (1982) discussed that such variation cannot be only due to different test conditions and devices used in the experiments and there has to be some specific factors (e.g. CO_2 pressure) which cause the variation of E_a and A.

2.1.4 Effect of partial pressure of CO_2

If the partial pressure of CO_2 in the system is low, the calcination reaction proceeds relatively fast to completion. By increasing the CO_2 concentration, the calcination reaction becomes slower, until the equilibrium CO_2 partial pressure over calcium carbonate is reached and limestone will no more decompose. In the literature, few correlations exist for the description of the equilibrium decomposition pressure of $CaCO_3$. Baker (1962) defined the equilibrium decomposition pressure according to equation (8):

$$\log P_{eq} = 7.079 - \frac{8308}{T}\ (atm). \quad (8)$$

Silcox *et al*. (1989) suggested the following equation (9):

$$P_{eq} = 4.137 \cdot 10^7 \exp\left(\frac{-20474}{T}\right) \text{(atm)}. \quad (9)$$

A comparison between the above mentioned correlations is shown in figure 2. By observing the graph it can be seen that the curves are nearly identical at low temperatures. The difference between the correlations is increasing at high temperatures (>850°C).

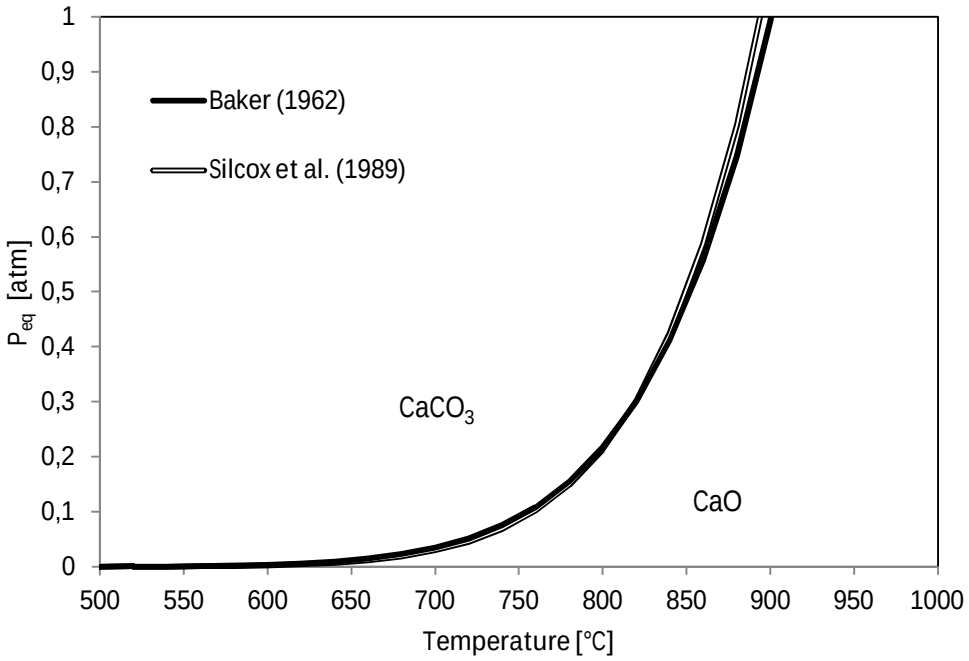

Figure 2 Equilibrium CO_2 partial pressure over $CaCO_3$.

When considering a single limestone particle, the effect of CO_2 on the calcination rate is complicated, since the CO_2 concentration is constantly varying inside the particle. Silcox *et al*. (1989) studied the calcination reaction in different CO_2 concentrations and ended to linear dependence, which is described with equation (10):

$$f\left(P_{CO_2}\right) = P_e - P_{CO_2}. \quad (10)$$

Later, Khinast *et al*. (1996) claimed that the effect of CO_2 partial pressure on the calcination rate is rather exponential than linear. In their study the equation (11) was suggested

$$f(P_{CO_2}) = \exp\left(-11.92 \cdot \frac{P_{CO_2}}{P_{eq}}\right). \quad (11)$$

However, the validation equation (11) was tested only for limited CO_2 concentrations in which the mole fraction of CO_2 at the reaction surface was $0 \leq x \geq 0.065$. According to Hu and Scaroni (1996) the dependence can be described with equation (12),

$$f(P_{CO_2}) = \left(1 - \frac{P_{CO_2}}{P_{eq}}\right), \quad (12)$$

if the partial pressure of CO_2 (in atm) is $10^{-2} \cdot P_{eq} < P_{CO2} < P_{eq}$. If in case the partial pressure of CO_2 is less than $10^{-2} \cdot P_{eq}$ it doesn't have effect on the reaction rate.

Later, García-Labiano *et al*. (2002) modified and tested the above mentioned equation as

$$f(P_{CO_2}) = \left(1 - \frac{P_{CO_2}}{P_{eq}}\right)^n. \quad (13)$$

In the work of Stanmore and Gilot (2005) it was discussed that one reason for the differing opinions about the CO_2 dependence could be that there are several ways to interpret the reaction interface and this also influences to the CO_2 dependence.

2.1.5 Effect of steam

Berger (1927) studied calcination reaction in dry air and in steam at different temperatures (650 °C, 700 °C, 800 °C, 900 °C and 1000 °C). In these experiments the calcination was always faster in steam than in dry air. Berger (1927) concluded that the differences observed were due to different physical properties of the gases and the way they affect to heat transfer from bulk gas to the limestone particle. Steam has neither catalytic, nor chemical effect on calcination.

Recently also Wang *et al*. (2008) carried out calcination experiments in CO_2/H_2O and CO_2/N_2 atmospheres and observed that the conversion in CO_2/H_2O mixture was always slightly higher than in CO_2/N_2 mixture. Just as Berger (1927), Wang *et al*. (2008) concluded that the difference was due to the different thermal conductivities of the gases. An example was given: according to Wang *et al*. (2008) the thermal conductivity of steam at 1193 is 0.127 W/(mK) and that of N_2 is 0.071 W/(mK).

2.1.6 Effect of particle size

The limestone particles fed to the calciner are typically large in size (d = 1–4 mm), but they are rapidly fragmented into smaller pieces (d = 75–500 μm) in the process conditions (García-Labiano *et al*. 2002, Mattisson and Lyngfelt 1998, I). At first, the fragmentation is caused by thermal stress and overpressure of CO_2 inside the particle. Secondary fragmentation occurs due to the collisions of the limestone particles which each other and with the calciner constructions. The attrition rate is high just after the sorbent feed but slows down to be quite steady in the end. (Scala *et al*. 1997, García-Labiano *et al*. 2002, Saastamoinen *et al*. 2008).

The residence time of the particle in the fluidized bed boiler depends on its size. It has been discovered, that particles with diameter less than 75 μm spend only seconds to few minutes in the boiler before they are drifted to the cyclone. Larger particles (100-200 μm) can instead have residence time up to several hours. (Mattisson and Lyngfelt 1998)

The size of the particles may also have an influence on the calcination rate by means of thermal and mass transfer. According to Hu and Scaroni (1996) this holds true especially for the larger particles; the calcination reaction causes higher CO_2 partial pressures within the particle which decelerate the calcination reaction. Since calcination reaction is endothermic, local colder zones exist near the reaction front which may reduce the reaction rate. Hu and Scaroni (1996) also concluded, based on their experiments at 1200 °C, that with very small particles (diameter of less than 10 μm) the temperature and CO_2 partial pressure gradients are negligible. Thus they suggested that small particles would be promising to obtain information about the reaction kinetics, since the reaction is only controlled by chemical reaction.

Also Khinast *et al*. (1996) studied the effects of particle size on calcination. Based on their experiments they concluded that particle size is an important parameter at low CO_2 concentrations, where the calcination occurs fast. However, at high CO_2 concentrations and the effect of particle size is instead diminished and the reaction rate depends mainly on the reaction surface area.

2.2 Carbonation

The carbonation (eq. 14) is the reaction which is used to capture the CO_2 from the flue gases. It is planned to carry out at atmospheric pressure and temperature range 600–700 °C.

$$CaO\ (s) + CO_2(g) \rightleftarrows CaCO_3(s) \tag{14}$$

The carbonation occurs in two stages; there is a rapid, chemically controlled initial stage but as the reactions proceeds a fast drop in the reaction rate is observed. This is due to a formation of solid $CaCO_3$ product layer on the surface of CaO particle which causes that diffusion of CO_2 through the product layer becomes rate controlling. The slow reaction rate enlarges the carbonator size and increases the dwell time. To achieve a reasonable CO_2 capture efficiency, only the fast reaction regime is suitable for operation. Unfortunately, the fast stage in carbonation lasts only some of minutes and thus different approaches (changes in gas composition, additives) are tested to improve the CO_2 capture capacity. (Abanades and Alvarez 2003, Sun *et al*. 2008 I, II).

2.2.1 Reaction kinetics

Several researchers have tried to investigate the reaction kinetics and determine an equation which describes the progress of the reaction. In the study of Bhatia and Perlmutter (1982), the mathematical discussion was divided to two parts: for the fast reaction regime the CaO conversion rate (*dX/dt*) is describe by the equation (15) and for the slow, diffusion controlled region by equation (16).

$$\frac{dX}{dt} = \frac{kC_{CO_2}S_0(1-X)\sqrt{1-\psi\ln(1-X)}}{1-\varepsilon_0} \quad (15)$$

$$\frac{dX}{dt} = \frac{kC_{CO_2}S_0(1-X)\sqrt{1-\psi\ln(1-X)}}{(1-\varepsilon_0)\left[1+\frac{\beta Z}{\psi}\left(\sqrt{1-\psi\ln(1-X)}-1\right)\right]} \quad (16)$$

In these above mentioned equations, ψ is a parameter which depends on initial surface area (S_0) per unit volume, porosity (ε) and the initial total pore length in system per unit volume (L_0), as described in the equation (17):

$$\psi = \frac{4\pi L_0(1-\varepsilon)}{{S_0}^2}. \quad (17)$$

The model is complicated to use because of the structural parameters (L_0, S_0, ε) which have to be determined empirically. (Lee 2004, Grasa *et al*. 2009)

Another widely used model is the shrinking core model, which is more simple to use than the above mentioned grain model. In the shrinking core model, the chemically controlled reaction is described by equation (18) and diffusion control by equation (19).

$$\frac{dX}{dt} = -\frac{kC_{CO2}}{\rho R}(1-X)^{\frac{2}{3}} \quad (18)$$

$$\frac{dX}{dt} = -\frac{6DC_{CO2}}{\rho R^2\left[3(1-X)^{-\frac{1}{3}}-2X\right]}. \quad (19)$$

Sun *et al*. (2008 I, II) suggested that the carbonation rate depends on the partial pressure of CO_2 as following:

$$k = 1.67\cdot 10^{-3}e^{\frac{-E_a}{RT}}, \qquad if\ P_{CO_2} - P_{eq} > 10\ kPa \quad (20)$$

$$k = 1.67 \cdot 10^{-4} e^{\frac{-E_a}{RT}}, \qquad if\ P_{CO_2} - P_{eq} < 10\ kPa\ , \tag{21}$$

where E_a = 29 ± 4 kJ/mol.

Alvarez and Abanadez (2005) also determined a critical thickness of the product layer which is the starting point for diffusion controlled reaction. According to their research, the critical thickness of the product layer is approximately 50 nm. As Grasa et al. (2009) stated, this can be interesting when studying the transition between the fast and slow reaction regime but doesn't provide enough information about the reaction rate before the product layer is formed nor for the design of the carbonator. Further research is needed and the development of modeling approaches should be continued. In the calcium looping applications, the system is even more complicated due to simultaneous carbonation–sulfation reactions.

2.2.2 Effect of temperature

The CO_2 capture efficiency depends on temperature and on the partial pressure of CO_2. High temperatures are beneficial when concerning reaction speed but at lower temperatures it is possible to achieve greater conversion (based on equilibrium). The optimum capture efficiency is found by balancing the two above mentioned. (Stanmore and Gilot 2005)

The effects of temperature on CO_2 capture have been studied recently by Lu *et al.* (2008) and Charitos *et al.* (2010). In the study of Lu *et al.* (2008), it was discovered that an optimum temperature range in the carbonator was approximately 580–600 °C with fresh CaO. If temperature was dropped to be less than 500°C, the carbon capture capacity drop remarkably and thus it was concluded that the reaction rate is too slow at temperatures below 500 °C. However, as the number of the sorbent cycles in the system increased, a higher temperature (~700 °C) is required for carbonation. This was explained to occur due the particle sintering and pore plugging. In the beginning of the reaction carbonation takes place in the small pores which have high surface area. As the reaction proceeds, the small pores are blocked and the penetration of CO_2 into the deep

pores is hindered. Thereafter, the reaction occurs mostly on the surface and in the bigger pores which have smaller surface area. However, by increasing the temperature, the diffusion of the gases is possibly enchanced and thus a higher temperature is better for carbonation after several cycles.

2.2.3 Effect of steam

To improve the sorbent activity and carbonation conversion, several approaches are tested. One of them could be steam addition, which was recently studied by Manovic and Anthony (2010). In their study, different limestones were tested and with most of them steam addition improved the carbonation conversion in the diffusion controlled stage. The enhancement in conversion was notable in lower temperatures (600 °C) but not in high temperatures (800 °C). It was explained that the higher temperature itself accelerates the diffusion, and thus the effects of steam are minimized in the higher temperatures. In addition, Manovic and Anthony (2010) noticed that steam injection is advantageous only for certain limit, because by increasing the steam concentration from 10% to 20%, the conversion to $CaCO_3$ was no more improved. Overall conclusions about the enhancing effects of steam are still difficult to make, since also exceptions in the behavior of different limestones were found: with limestones Cadomin and La Blanca water vapor didn't improve the conversion. It was discussed that probably the chemical composition of these limestones (e.g. sodium ions, which may enhance the solid state diffusion so that the effect of water vapour becomes negligible) or physical structure were responsible for the observed differences.

2.3 Sulfation

Sulfur enters to the calcium looping process in two ways: SO_2 comes along the flue gases which are conducted to the carbonator, second source is the calciner where coal is burned to ensure a sufficient temperature for the calcination reaction. In the system, sulfur forms mainly $CaSO_4$, with direct sulfation (eq. 22) or indirect sulfation (eq. 23–24), depending on the process conditions. (Anthony and Granatstein 2000, Blamey *et al.* 2010, Manovic and Anthony 2010)

$$CaCO_3(s) + SO_2(g) + \frac{1}{2}O_2(g) \rightarrow CaSO_4(s) + CO_2(g) \quad (22)$$

or

$$CaCO_3 \rightarrow CaO + CO_2 \quad (23)$$

$$CaO(s) + SO_2(g) + \frac{1}{2}O_2(g) \longrightarrow CaSO_4(s) \quad (24)$$

If the partial pressure of CO_2 in the system is greater than the equilibrium decomposition pressure of calcium carbonate, limestone doesn't decompose and direct sulfation occurs (figure 3). Correspondingly, indirect sulfation occurs when the partial pressure of CO_2 is less than the decomposition pressure of calcium carbonate, allowing limestone to calcine before sulfation. In normal air-fired FBC, calcination–sulfation is governing whereas in pressurized systems and in the oxy-fuel and calcium looping cycle limestone can be directly sulfated, since the partial pressure of CO_2 is typically around 0.7 or more and can exceed the equilibrium pressure (Myöhänen *et al.* 2009).

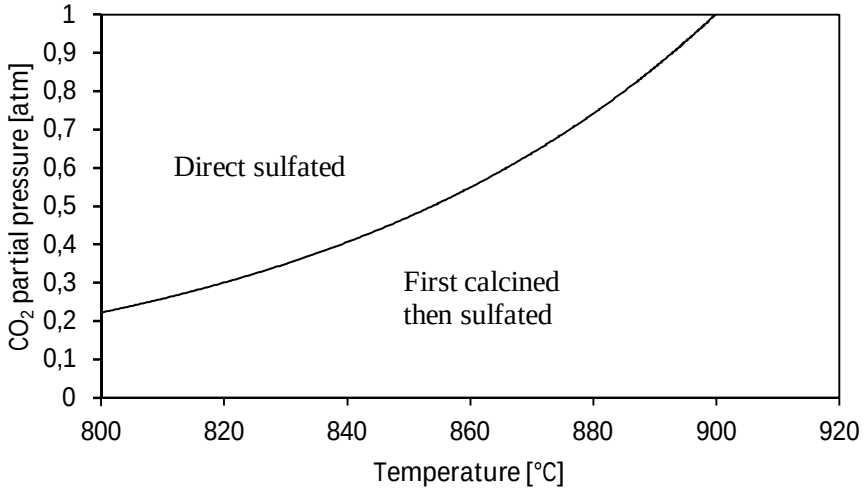

Figure 3 Sulfation occurs either with direct sulfation or with calcination–-sulfation chemistry depending on the equilibrium decomposition partial pressure over $CaCO_3$. (Zhao *et al.* 2010 p. 52)

2.3.1 Diffusion

The indirect sulfation is described to occur in two stages. In the beginning of the reaction, both chemical reaction and the gas diffusion of SO_2 and O_2 in the pores can be rate limiting. As the reaction proceeds, a non porous $CaSO_4$ product layer is formed on the surface of the particle. The molar volume $CaSO_4$ is greater than that of CaO which leads to pore blockage. This causes that diffusion through the product layer becomes rate limiting and the reaction becomes extremely slow. Typically only 30–40% conversion of CaO to $CaSO_4$ is observed in AFBC. However, there can be notable differences in Ca utilization depending on the limestone porosity, particle size, residence time, microstructure, purity and process conditions. (Laursen et al. 2000)

When concerning direct sulfation, differences have been found. First observation is that that the reaction occurs more slowly than indirect sulfation. This is explained by the smaller porosity and smaller specific surface area of reacting $CaCO_3$ than those of CaO. Secondly, the diffusion coefficient in the product layer in direct sulfation is higher than in the indirect sulfation. The reasons for this is still unclear, some researchers have explained that it is the counter diffusion of CO_2 that keeps the product layer porous, while others claim that it is the nucleation and formation of crystal grains. Whatever the truth, the smaller diffusion resistance may lead to situation that greater conversion to $CaSO_4$ can be achieved with direct sulfation than with calcination–sulfation chemistry if the residence time of the particle in the boiler is long enough.

The determination of the diffusion coefficients is difficult with laboratory measurements and that is why modeling could be a useful tool for this purpose. But, as Adanez *et al*. (2000) stated, different models seem to predict different diffusion coefficients, possible due to different assumptions which are made in the modeling. Hu *et al*. (2006) gathered values for effective diffusion coefficients used for direct sulfation from different authors and noticed that values ranging from 10^{-6}–10^{-15} m^2/s were used at temperature 1123 K.

For the understanding of the sulfation phenomena as well as for process design it is important to understand what is the rate limiting factor in each stage of the reaction. For the evaluation, Thiele modulus can be used: it describes the relation of reaction rate to diffusion speed. If the value of Thiele modulus is much higher than 1, then the

intraparticle diffusion is limiting factor. When 0.1 < Thiele < 10, both chemical kinetics and diffusion are limiting. And if the value of Thiele modulus is much smaller than 1, then reaction kinetics is the controlling mechanism. The Thiele modulus is presented in equation 25:

$$\Phi_m = L\left(\frac{k}{D_{eff}}\right)^{1/2} \tag{25}$$

where

L	shape factor.
k	reaction rate coefficient
D_{eff}	effective diffusion.

For a arbitrary shaped particle, L is

$$L = \frac{V}{A_s}, \tag{26}$$

where

V	volume of the particle
A_s	outer surface area of the particle

and for a sphere

$$L = \frac{R}{3}, \tag{27}$$

where

R	particle radius.

2.3.2 Reaction kinetics

The rate expressions for direct sulphation are typically given in a form:

$$r = k(T){C_{SO2}}^{n}, \qquad \text{mol}/(\text{m}^2\text{s}) \tag{28}$$

where

r	reaction rate for direct sulfation
k	reaction rate constant, depends on temperature
C_{SO_2}	concentration of SO_2
n	reaction order.

By this far, researchers are not in agreement with the reaction order of SO_2 and values varying from 0.4 to 1 have been suggested. Typically the effects of O_2 and CO_2 have been ignored.

When concerning indirect sulfation, the rate expressions are very similar. For example Borgwardt (1986) suggested for sulfation reaction rate

$$r = 2.65 \cdot S^2 \cdot P_{SO_2}^{0.64} \exp\left(-\frac{36600}{RT}\right). \tag{29}$$

Normally only linear expressions are used, but Mattisson and Lyngfelt (1998, I) apply an exponential decay function where the rate is decreasing as the sulfation reaction proceeds:

$$r_s = P_{SO_2}^{n} \cdot c_1 \cdot exp(-c_2 \cdot X_{CaSO_4}). \tag{30}$$

In equation (30) c_1 and c_2 are fitting parameters.

2.3.3 Effect of temperature

In fluidized bed combustion, the sulfur capture capacity depends on temperature. For air-fired units, it has been observed that an optimum temperature range exist for sulfur capture, being approximately 850–870 °C. If the temperature is higher than the optimal sulfur capture temperature, sintering increases, which leads to smaller specific surface area, smaller porosity and bigger grain size of the reacting solid. Another reason for

reducing sulfur capture might be the desulfation reactions which occur more likely in higher temperatures.

It has been suggested that also in O_2/CO_2 atmosphere optimum temperature exist for sulfur capture, but it is much higher than in air. Chen and Zhao (2006) examined the sulfur capture capacities in temperature range 800-1200 °C in CO_2/O_2 atmosphere (80% CO_2, 3000 ppm SO_2, O_2 as balance) and in air (3000 ppm SO_2) and concluded that the optimal temperature for sulfur capture in CO_2/O_2 atmosphere was around 1050 °C which allowed calcination–sulfation chemistry. It was explained that in the high temperatures of CO_2/O_2 atmosphere calcination occurs slowly but produces nascent CaO for longer period than in air. In these conditions also the pore structure is different and may lead to higher Ca –utilization in than in air.

Also García-Labiano *et al*. (2011) studied the effects of temperature on sulfur capture. In the study of García-Labiano *et al.* (2011) atmosphere containing 60% CO_2 was used and temperatures 800-975 °C were tested. The highest conversions were achieved with calcination–sulfation chemistry at 900 °C. By increasing the temperature up to 975 °C, conversion to $CaSO_4$ decreased. At the lower temperatures (800-850 °C) where direct sulfation occurred, the conversion to $CaSO_4$ was always smaller during the test time.

2.3.4 Effect of O_2 concentration

On theoretical bases, both sulfation reactions would depend on O_2 partial pressure (concentration) in addition to $\sqrt{p_{SO_2}}$. However, in air-fired units the reaction order of O_2 is often considered to be zero, possibly because the O_2 concentration is much higher than SO_2 concentration and thus it is likely that it is the SO_2 concentration which is rate limiting. Liu *et al*. (2000) concluded that if O_2 concentration is more than 5%, it has negligible effect on sulfation degree. On the other hand, Dennis and Hayhurst (1990) claimed that the O_2 doesn't have effect on the initial reaction rate but it can instead affect the indirect sulfation in the diffusion controlled region.

When considering direct sulfation, Hu *et al*. (2007) noticed that O_2 concentration increased the reaction rate of direct sulfation up to concentrations 15% O_2. In these cases the reaction order was found to be 0.4. Duan *et al*. (2011) carried out experiments 50kW_{th} CFB apparatus, and noticed that the desulfurization efficiency was improved

with both direct sulfation and calcination/sulfation by elevating the O_2 concentration. According to Duan *et al*. the main effect of the O_2 concentration is that it reduces the reductive conditions in the boiler.

2.3.5 Effect of water vapor

To improve the sorbent utilization and desulfurization efficiency, several methods have been suggested. One of them is hydration, since it has been observed that water can permeate through the $CaSO_4$ product layer and react with CaO to form $Ca(OH)_2$. The formation of $Ca(OH)_2$ may cause cracks on the sulfate cover, because the molar volume of $Ca(OH)_2$ is greater than that of CaO. The hydration reaction is likely to occur in relatively low temperatures (< 600 °C), because $Ca(OH)_2$ is not thermodynamically stable at high temperatures. Thus it has been discussed of adding a sorbent regeneration step to the looping process and after the hydration, the particles would be re-injected to the boiler. However, this method would decrease the thermal efficiency (low hydration temperature) and require severe modifications to the process. (Laursen *et al*. 2000)

Nevertheless, in the laboratory scale tests (e.g. Hajaligol *et al*. (1988), Hu *et al*. (2007), Steward *et al*. (2010), Wang *et al*. (2010), Wang *et al*. (2011)), it has been observed that water vapor has an promoting effect even at high temperatures and on both, indirect and direct sulfation. The enhancement was significant in the diffusion controlled area rather than in the beginning of the reaction, where chemical reaction is rate limiting.

The mechamism of sulfation in atmosphere containing steam is not yet fully understood, but for example Wang *et al*. (2010) used the following reactions (31–32) to explain the test results:

$$CaO\ (s) + H_2O(g) \longrightarrow Ca(OH)_2(s) \tag{31}$$

$$Ca(OH)_2(s) + SO_2(g) + \frac{1}{2}O_2(g) \longrightarrow CaSO_4(s) + H_2O(g). \tag{32}$$

Wang *et al*. (2010) claimed that water vapor acts as a catalyst in the process. Part of the CaO in the process could form $Ca(OH)_2$ and the formed $Ca(OH)_2$ reacts faster with SO_2 than CaO. Later, Steward *et al*. (2010) argued this explanation, noting that if in case

$Ca(OH)_2$ is formed and it reacts with SO_2 faster than CaO, it should also affect to the chemically controlled region. Thus, Steward *et al*. (2010) claimed that H_2O doesn't take part in the sulfation reaction itself but it instead affects to the diffusion of the gaseous reactants and/or to the solid-state diffusion mechanism. Steward *et al*. (2010) also discussed, that it seems that an optimum H_2O concentration exists for sulfur capture, because the sulfate conversion was no more improved with H_2O concentrations more than 30 %.

2.3.6 Reducing conditions

Though direct and indirect sulfation are the main sulfur related reactions, formation of other chemical species such as $CaSO_3$ and CaS is possible. The occurrence of different species depends on oxidizing/reducing conditions, on the temperature, and on the composition of the fuel (Anthony and Granatstein 2001).

In fluidized beds, the reducing conditions may occur in the dense bed or near the walls. Also air-staging or uneven fuel feed may cause reducing zones. Actually, in industrial scale boilers, the conditions can be periodically changing between oxidizing and reducing. This may affect significantly to the sulfur capture efficiency, either an increase or a decrease in the final conversion is possible, depending on the on the time under the reducing conditions.

Mattisson and Lyngfelt (1998, II) discussed that especially CO and H_2 may cause decomposition of calcium sulfate according to reaction (33):

$$CaSO_4(s) + CO/H_2(g) \rightarrow CaO\,(s) + SO_2(g) + CO_2/H_2O\,(g). \quad (33)$$

According to their research, it is also possible that CaS is formed in the reductive conditions either from $CaSO_4$

$$CaSO_4(s) + 4CO(g) \longrightarrow CaS(s) + 4CO_2(g) \quad (34)$$

or from CaO:

$$CaO(s) + 3CO(g) + SO_2(g) \longrightarrow CaS(s) + 3CO_2(g). \quad (35)$$

The formed CaS may also react with $CaSO_4$ and release SO_2 at temperatures above 900°C

$$CaS(s) + 3CaSO_4(s) \rightarrow 4CaO(s) + 4SO_2(g). \quad (36)$$

If the conditions are highly reducing, then it is likely that the sulfur compounds form hydrogen sulfide (H_2S) or carbonyl sulfide (COS) instead of SO_2. Both H_2S and COS can react with CaO forming CaS, according to the reaction (37).

$$CaO(s) + H_2S/COS\,(g) \rightarrow CaS(s) + H_2O/CO_2(g). \quad (37)$$

The molar volume of CaS is smaller than that of $CaSO_4$ and thus the diffusion resistance through the CaS product layer is smaller. This means that in highly reducing conditions the calcium utilization can be greater than in air-fired units.

The above mentioned equations can be valid for real industrial scale boilers. However, in laboratory scale tests it is common that fuel is not fed to the boiler and the temperature is adjusted with electrical heaters. In these conditions the reducing agents, CO, H_2 and CH_4 do not exist.

Dennis and Hayhurst (1990) studied the sulfation reaction in laboratory scale apparatus with was electrically heated noticed that sulfure capture occurred even in atmosphere containing 0 % oxygen. In these conditions the initial sulfation rate was same as in the higher O_2 concentrations. Dennis and Hayhurst concluded that sulfation is a very complex phenomenon and may include the following reactions:

$$CaO + SO_2 \rightarrow CaSO_3 \quad (38)$$

$$4CaSO_3 \rightarrow CaS + 3CaSO_4 \quad (39)$$

$$CaS + 2O_2 \rightarrow CaSO_4. \quad (40)$$

In this reaction series it is suggested that CaO reacts directly with SO_2. The formed $CaSO_3$ is unstable in the process conditions and thus it decomposes rapidly to other reaction products (CaS and $CaSO_4$). Finally, if oxygen is available, CaS is oxidized, so that the end product is always $CaSO_4$.

3 PARTICLE MODELS

To understand the complicated reaction kinetics and rate limiting factors, particle models have been created. These models observe a single limestone particle in the process as a function of time, and the progress of the reactions. All reactions that occur in the looping cycles are heterogeneous gas–solid reactions which take place in the porous structure of the limestone particle. Regardless of the model chosen, the fundamentals of the modeling involve chemical reactions, mass and heat transfer rates through the particle and mass and heat transfer from the particle surface to the bulk gas.

Typically, four types of models are used to predict the progress of the reactions: shrinking core models, grain models, pore models and volume reaction models. It is commonly assumed with all the models that the limestone particle is spherical, isothermal and that the pseudo-steady approximation can be done. A general problem is that although many models give a good estimate for certain limestone type and size they cannot be generally used for different limestone types. This is due to the fact that huge differences in the reaction rates as well as in the limestone's properties have been discovered, depending on their origin. The pore structure and porosity may vary greatly, e.g. initial porosity values between 0.03 and 0.3 have been measured. In addition, the limestone particle's fragmentation is case-specific since each limestone supports differently the high temperatures and mechanical stresses which appear in the boiler. In some cases also the chemical composition (e.g. contents of Al_2O_3, SiO_2 and Fe_2O_3) may have an effect on the reactions. (García-Labiano *et al.* 2002, Adánez *et al.* 2006, Mattisson and Lyngfelt 1998, I)

3.1 Shrinking core model

The shrinking unreacted core model is the most frequently used model when considering sulfation reactions. The main advantage of this model is its simplicity. In the shrinking core model it is assumed that the reaction starts from the surface of the particle and proceeds with constant reaction rate towards the center. The particle is assumed to be homogeneous and there is a sharp interface between the product layer and fresh reactant. The amount of unreacted core is reducing, shrinking, as the reaction proceeds. The particle is assumed to be isothermal and spherical. In many cases fragmentation and attrition are not considered, which means that the diameter of the

particle is constant and that there are no changes in the particle shape. However, the shrinking core model is not applicable in all cases i.e. when the reaction is slow and the particle is very porous, neither in cases where a solid matter reacts only due to heat without a gas reactant, such as calcination for example. In addition, the shrinking core model doesn't consider the porosity of the particle and assumes that the composition of the gas phase surrounding the particle does not change. (Levenspiel 1999)

3.2 Grain models

In the grain models the particle is assumed to consist of a group of small grains which are spherical and nonporous. The space between the grains can be referred as the porosity of the particle. The gases move between the grains and react with them. Typically the grains are assumed to react according to the shrinking core mechanism. The grain models have been used to study both calcination (e.g. García-Labiano *et al*. 2002) and sulfation reactions (e.g. Dam-Johansen *et al*. 1991).

3.3 Pore models

The pore models assume that the pores of the particle are rectangular in shape. Both single pore size and distributed pore size models are used. Some models also consider the overlaps of the pores. The gases diffuse into the pores and react with the solid material. The formation of the product layer causes that pores start to block gradually until the reactions are totally prevented. (Andanez *et al.* 2000, Stanmore and Gilot 2005)

3.4 Volume reaction models

In the volume reaction methods, the particle is divided into control-volumes and the transport equations for fluid flow and heat transfer are written to each finite volume. The differential equations are solved numerically by means of modeling. Typically only diffusion is considered to be the transport mechanism inside the particle, but e.g. Khinast *et al.* (1996) and Takkinen *et al*. (2011) included advection term into their model. The diffusion of the gases inside the particle is random, but the net flow of the gases is from greater concentration towards the smaller one. Advection describes the mass transfer of moving CO_2 flow and depends on the pressure gradient. (Versteeg and Malalasekera 1995, Shiravani *et al*. 2008)

On the outer surface of the particle, the mass and heat transfer is different compared to the inner parts of the particle, since the fluid flow passing by the particle affects to transfer rates. For the calculation, several correlations have been developed and the calculation is done with aid of dimensionless parameters. The mass transfer rate on the surface is typically calculated from Sherwood's number:

$$Sh = \frac{h_m d}{D} = f(Re, Sc), \tag{41}$$

in which

h_m	mass transfer coefficient
d	diameter of the particle (particle is assumed to be spherical)
D	diffusion coefficient
Re	Reynolds number
Sh	Sherwood number.

One of the most commonly used correlation is the Frössling's equation:

$$Sh = 2.0 + 0.69 \cdot Re^{1/2} Sc^{1/3} \tag{42}$$

which can be used for flow passing a single sphere. If in case the particle is very small and the gas velocity is small, then is also possible to use an assumption that $Sh = 2$, which is the smallest possible value. Some researchers have also considered the effect of packet bed on the fluid flow, in these cases the mass transfer depends on the voidage (ε) of the inert bed material as described in equation 43: (Hayhurst and Parmar 2002)

$$Sh = 2\varepsilon + 0.69(Re/\varepsilon)^{0.5} Sc^{0.3}. \tag{43}$$

To estimate the heat transfer on the particle surface, dimensionless Nusselt number is used:

$$Nu = \frac{hd}{k} = f(Re, \mathrm{Pr}) \tag{44}$$

where

h	heat transfer coefficient
d	diameter of the particle (particle is assumed to be a sphere)
k	thermal conductivity.

For a sphere, the typically used correlation is

$$Nu = 2 + 0.60 \cdot Re^{1/2} Pr^{1/2}. \tag{45}$$

4 MATERIALS AND METHODS

In this study, three different methods were used to study the limestone reactions. The sulfur capture experiments were carried out in a bench scale BFB test device and the effects of temperature and gas composition i.e. sulfur and oxygen concentration was studied. The laboratory test results were analyzed and compared with numerical particle model simulations. Finally the structure and composition of a limestone sample was studied with aid of SEM-EDS analysis.

4.1 Laboratory tests with bench-scale fluidized bed

In the laboratory tests, a bubbling fluidized bed was used. The schematic structure of the apparatus in represented in figure 4. The height of the reactor was 669 mm and the inner diameter of the reactor (upper part) was 53.1 mm. The inner diameter of the lower part of the reactor (just above the grid) was 36 mm. (Takkinen *et al*. 2011)

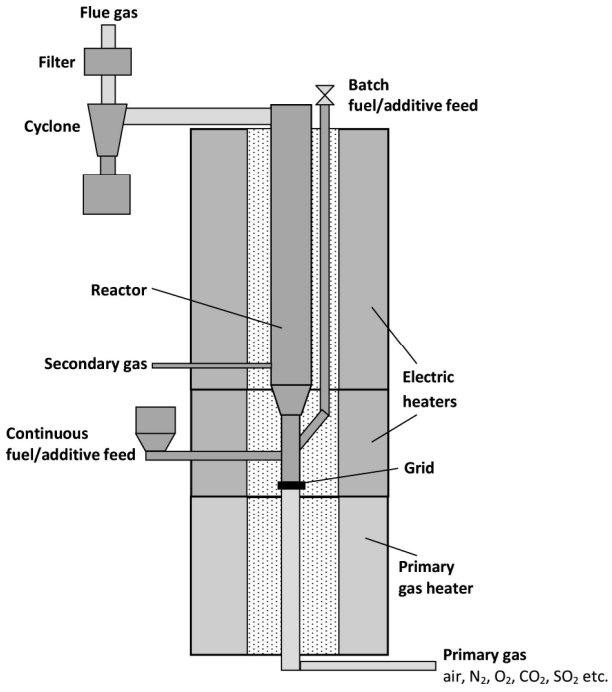

Figure 4 Test device (Takkinen *et al.* 2011).

The temperature of the reactor was adjusted with electric heaters which were surrounding the reactor. To ensure the right temperature profile in the reactor, the temperature was measured in six different places of the test device. The gas fed to the reactor was preheated before it passed through a perforated grid. The SO_2 was mixed

with other gases before the gas heater. Later, it was realized, that a small part of SO_2 could react with O_2 forming SO_3 in the gas heating tubes. Thus, few extra tests with a different SO_2 feed arrangement were done, but the differences between the measured calcium utilisation rates were not significant.

For the sulfure capture, a commercial limestone (Nordkalk GE500KO) which composed of 95% calcium carbonate ($CaCO_3$) and 5% of inert material was used. The particles were sieved to size fractions of 125-500 µm and in each tests, 1 g of limestone was fed to the boiler. The bed sand mass was 24 g during the tests. The escape of fine particles was measured and it was found out to be negligible (less than 5%). The flue gas flow escaping the reactor was measured with online gas analyzers and the calcium use was calculated by integrating the gas responses.

4.2 Numerical particle model

To examine the limestone reactions, a numerical, one-dimensional particle model was used. With aid of this model, it is possible to study the calcination, carbonation and sulfation (indirect and direct) reactions simultaneously.

In the model, following assumptions have been done:

1. the particle is spherical
2. the shape and diameter of the particle does not change during the process
3. all the gases in the system are assumed to be ideal
4. a uniform value for effective diffusivity has been assumed for all the gaseous species.

The gas media in the model can be adjusted, and it includes N_2, O_2, CO_2 and SO_2 and mixture of theirs. The solid components which are considered in the model are $CaCO_3$, CaO and $CaSO_4$.

The calculation is divided into elements in the direction of the radius as described in figure 5. The mass and heat transfer equations are written for each element on the basis: change = flow in – flow out + source, where the source term refers to the mass source of a chemical component or to the change in formation energy due to chemical reactions.

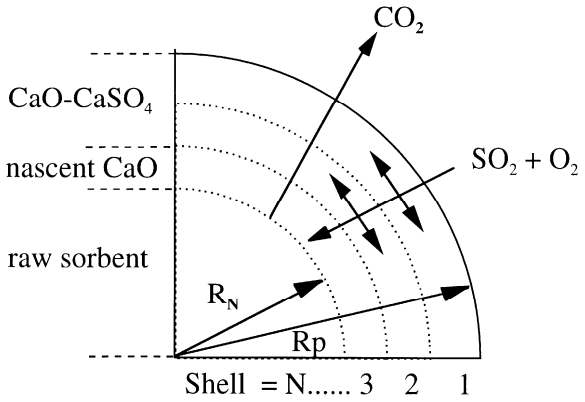

Figure 5 The particle is assumed to be spherical and for calculation the particle is divided into elements. (Adánez *et al*. 2000, p. 3668).

When considering the mass transfer in the gas phase inside the particle, diffusion is considered. The source term (S_i) either consumes (SO_2, O_2) or generates (CO_2) gas in each element.

$$\frac{d}{dt}\int_V \varepsilon_g \rho_p Y_i dV = -\oint_A \left[-\varepsilon_g \rho_g \mathrm{D}_{\mathrm{eff}} \nabla Y_i\right] \boldsymbol{n}\, dA + \int_V \upsilon_i S_i dV, \tag{46}$$

The amount of solids is calculated on the base mass in the beginning + source (47):

$$\frac{d}{dt}\int_V \varepsilon_s \rho_s Y_h dV = \frac{M_{product}}{M_{reactant}} \int_V S_i dV. \tag{47}$$

In the energy equation, two factors are taken into account: conduction of heat and reaction enthalpy as written in the equation (48).

$$\frac{d}{dt}\int_V \rho_{tot} c_p T dV = \oint_A \left[k_{eff} \nabla T\right] \boldsymbol{n}\, dA + \int_V \Delta H S_m dV. \tag{48}$$

In this case the porosity of the limestone was not known but it was estimated to be 0.3, since the reactions occurred fast. The initial size fraction of the particles used in laboratory tests was 125-500 µm but because it is known that particles can be

fragmented after they are fed to the boiler (e.g. Saastamoinen *et al*. 2008), a particle size of 110 µm was chosen for the modeling.

The principle for the source terms were taken from Takkinen *et al*. (2011). However, in this case modifications were needed, because a great difference in the reaction rates were observed. In the study of Takkinen *et al*. (2011) a stationary stage in sulfure capture was achieved in 1.5–2.0 hours whereas in the current study, the stationary stage occurred approximately in 10 minutes. It was concluded that so remarkable differences in the conversion rates were due to different limestone structure. Possibly, in the study of Takkinen *et al*. (2011) the limestone was very dense and the pores were formed in such a way that the movement of the gases was inhibited and as a result a small diffusion coefficient as well as a slow reaction rate was observed. With the current case, it could be possible that particle was highly cracked and the diffusion of the gases was occurring in large gaps instead of solid material diffusion.

With the diffusion coefficients large uncertainly exits, because there is no exact theory which would enable the calculation of the diffusion coefficients in a porous media. Further, the estimation of the diffusion coefficients is complicated by the fact that each gas has its own value and that the diffusion coefficients can vary remarkably depending on temperature and total pressure of the system. According to Cussler (1997) the gas-diffusion coefficient (at one atmosphere) for air–O_2 gas pair is $1.76 \cdot 10^{-5}$ m^2/s at 0 °C and for N_2–SO_2 gas pair $1.04 \cdot 10^{-5}$ m^2/s at -10 °C. However, Cussler also mentioned that generally, for example an increase of 300 K triples the coefficients. Thus it can be concluded that in high temperatures, as in the boilers (850–950 °C), the diffusion of the gases may be greatly enhanced, and values as high as $1 \cdot 10^{-4}$ m^2/s are possible. Of course these above mentioned values are for free gas flow which is not limited by the porous structure of the limestone particle. Thus the effective diffusion coefficient should always be smaller than the gas diffusion coefficient.

The correlations used in this study are described in table 1. The kinetic and diffusion parameters are chosen to fit the tests results as well as possible. The value of the effective diffusion is very high, it could possibly describe the diffusion in gas phase but is unrealistic value for solid state diffusion. Nevertheless, in this study it was thought that in a very porous and partly fractioned limestone structure the gas flow was not

significantly inhibited, at least in the beginning of the reaction when the nonporous $CaSO_4$ product layer was still thin.

Table 1 Correlations used in the modeling.

Calcination	$8 \cdot (-2 \cdot 10^{-6}T + 0.002808)(P_{eq} - P_{CO_2})(Y_{CaCO_3})$
Sulfation	$900 \cdot x_{SO_2} Y_{CaO}$
Diffusion	$Y_{CaSO_4} < 0.11, \quad D_{eff} = 7.8 \cdot 10^{-5}$ $Y_{CaSO_4} \geq 0.11, \quad D_{eff} = 2 \cdot 10^{-14} \cdot {Y_{CaSO_4}}^{-10}$

4.3 SEM-EDS analysis

The SEM-EDS equipment can be used study the surface structure and chemical composition of solid samples. In the apparatus, an electron beam is focused on the sample. The collisions of the primary electrons with the sample produce secondary electrons and back-scattered electrons which are used for the picture formation. The scanned sample also emits X-rays which can be used for the elemental analysis.

In this work a scanning electron microscope (JEOL JSM–5800) was used to study the structure and characteristics of uncalcined and sulfated samples of Endesa limestone. For the analysis, the samples were pretreated in two different ways. One part was kept un-embedded and only coated with gold before the SEM analysis. The other part of the limestone particles was embedded in epoxy (bisphenol-A-epichlorhydrin epoxy resin), cross-sectioned and polished with water before the analysis. In this case the effect of water was estimated to be small, although it is known that water might have interactions with the sample.

The local sulfation degree ($CaSO_4$ conversion level) of specified areas in the cross-sectioned samples was estimated by using equation (49)

$$X_{CaSO_4} = \frac{M_{Ca} W_S}{M_S W_{Ca}}, \tag{49}$$

where

M_i molar mass of element i
W_i weight percentage of element i.

5 RESULTS AND DISCUSSION

The discussion is divided into five parts. The first part examines a case where a sulfur capture test was carried out in air with 2000 ppm SO_2. In the following cases, the effects of process conditions, i.e. the effect of a smaller sulfur concentration, the effect of temperature and the effect oxygen concentration on sulfure capture are taken into consideration. In the last part, the surface structure and sulfation characteristics of a limestone are studied with aid of the SEM-EDS analysis results.

5.1 Simultaneous calcination–sulfation

A sulfur capture experiment was carried out in air at 850 °C and the SO_2 concentration in the test was 2000 ppm. In these conditions the limestone was first calcined and then sulfated to approximately 30% $CaSO_4$ conversion level which is typical for air-fired atmospheric units. A comparison between the laboratory test and modeled values are shown in figure 6.

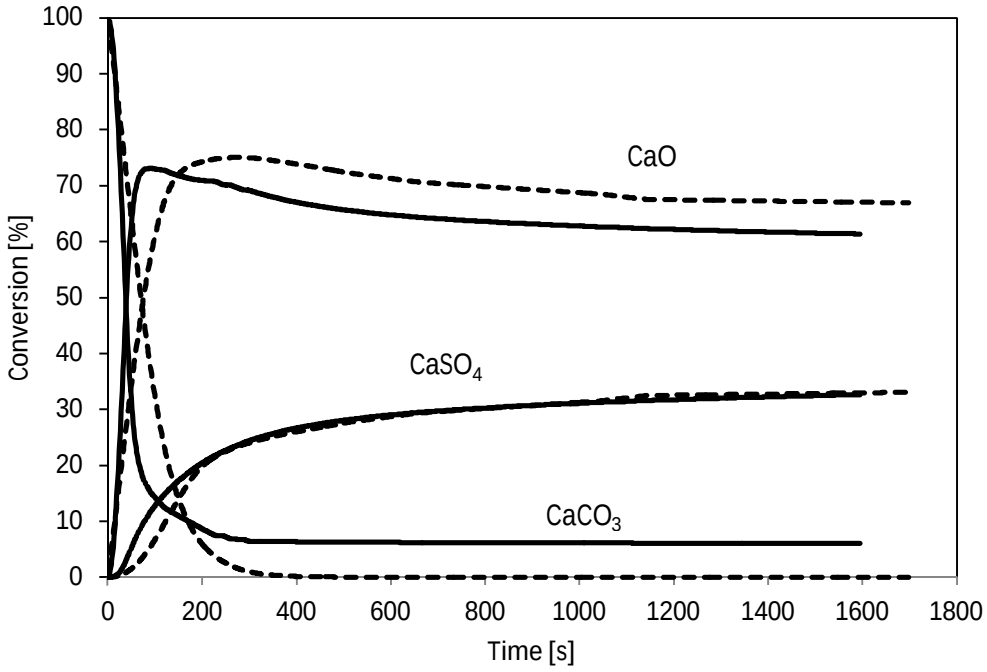

Figure 6 Simultaneous calcination and sulfation at 850°C. The laboratory tests are marked with (—) and modeled with (--).

By observing the graph it can be seen that there is a moderate correspondence between the laboratory results and modeled values, although clear differences exist. A major divergence is noticed with calcination reaction. In the laboratory test it was observed that approximately 6% of the $CaCO_3$ fed to the system didn't calcine, but in the modeling, the particle was allowed to calcine fully. This was done, because it was noticed that as the diffusion coefficient diminished, the CO_2 partial pressure inside the particle increased gradually until it exceeded the equilibrium decomposition pressure over $CaCO_3$, indicating that carbonation would occur inside the particle. This didn't seem likely, it would be more reasonable that the particle would fragment into smaller pieces if the partial pressure of CO_2 is high. However, it was noticed in the modeling that if the particle was allowed to calcine fully, the partial pressure of CO_2 inside the particle was notably smaller and didn't exceed the equilibrium pressure. The parameters which had described the progress of reaction with more accurate level were not able to find during this study.

Figure 7 shows the modeled $CaSO_4$ mass fractions in some parts of the particle as a function of time. From this graph it can be seen, that in the beginning of the reaction the sulfate formation was nearly uniform inside the particle. As the reaction proceeded, a thick sulfate layer was formed to the outermost shell.

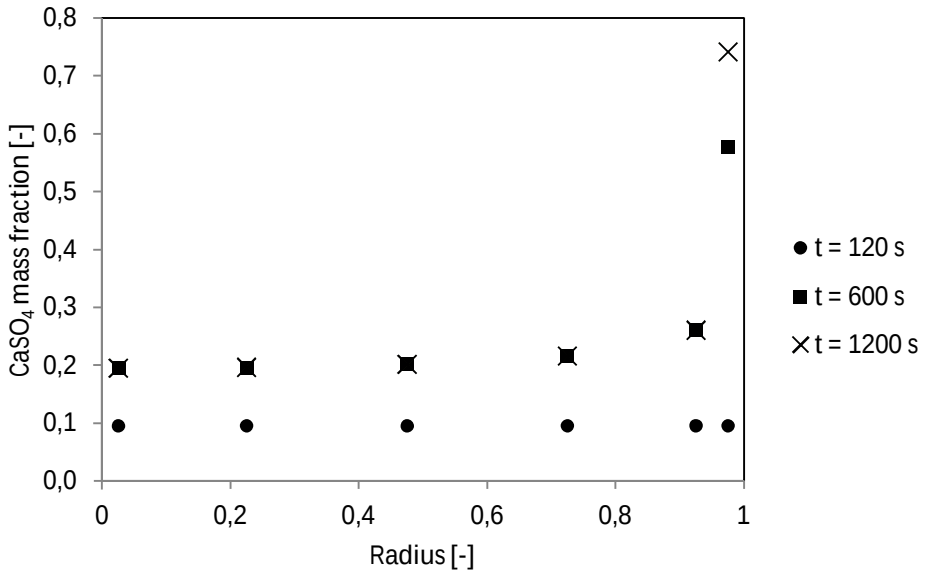

Figure 7 The modeled $CaSO_4$ mass fractions in the two outermost elements as well as some inner parts the particle at different times at 850°C (air with 2000 ppm SO_2).

The same conclusion can be drawn from figure 8, which describes the development of the local diffusion coefficient inside the particle. In the beginning of the reaction the diffusion coefficient was assumed to be constant. Since a high initial value was chosen, the sulfation rate was nearly uniform inside the particle during the first 200 s. As the diffusion coefficient started to diminish, the inflow of SO_2 to the particle was hindered, until the sulfation reaction stopped in the inner parts of the particle. After 400 s the diffusion resistance through the $CaSO_4$ product layer was so high that it was only the outermost rim of the particle that sulfated, causing the great decrease in the diffusion coefficient.

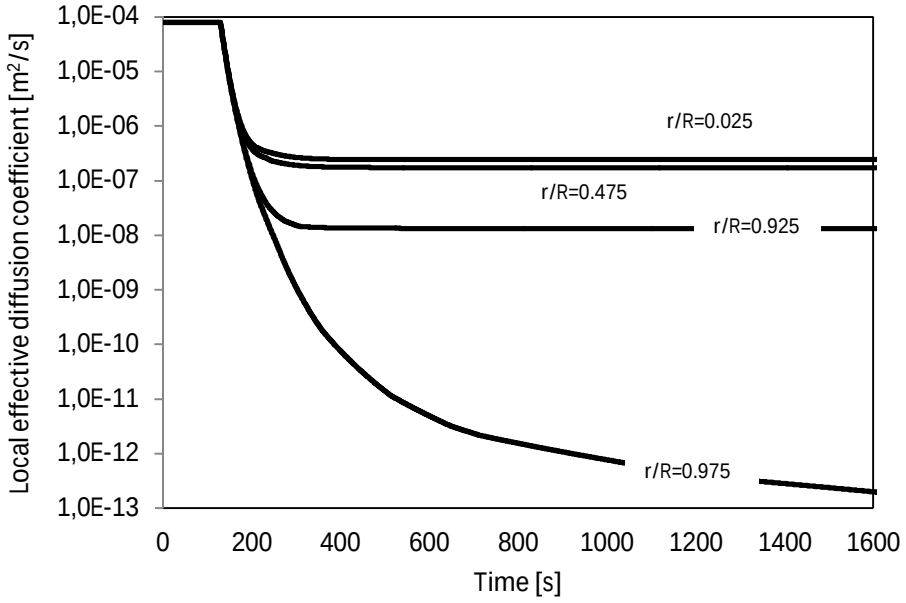

Figure 8 Development of the local effective diffusion coefficient inside the particle at 850C (air with 2000 ppm SO_2)

For the understanding of the sulfation phenomena as well as for the process design it is important to know what is the rate limiting step in each stage of the sulfur capture. In this study, the rate limiting mechanism was estimated with aid of Thiele parameter, Φ_m. The development of the Thiele parameter is shown in figure 9. From this figure it can be seen that in the beginning of the reaction, chemical kinetics were controlling, since $\Phi_m = 0.06$ (< 0.1). As the reaction proceeded, the significance of the diffusion was emphasized, until in the end the reaction was limited only by diffusion and $\Phi_m > 10$.

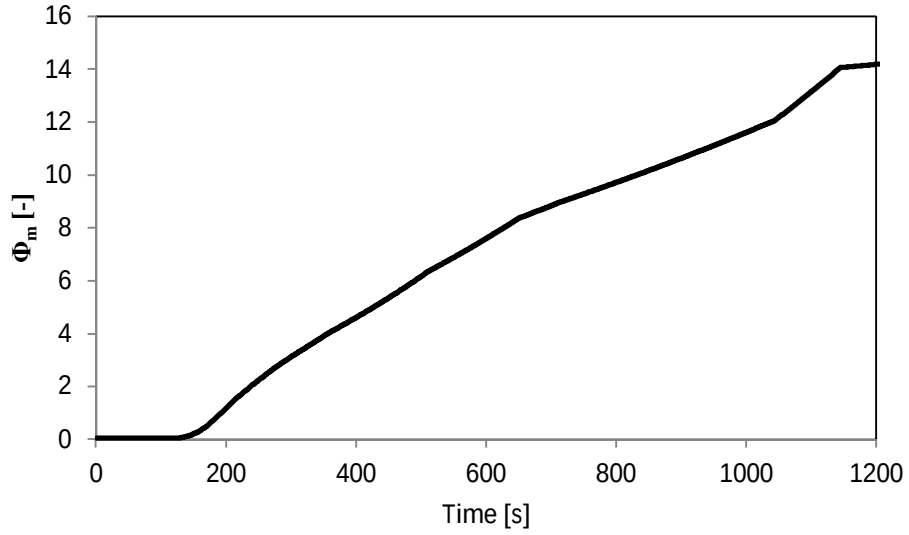

Figure 9 Development of Thiele modulus for sulfation in air at 850°C .

5.2 Effect of SO_2 concentration

It is well known that sulfure capture is greatly affected by the SO_2 concentration. In the laboratory tests, two different SO_2 concentrations were tested, air with 1000 ppm SO_2 and air with 2000 ppm SO_2. As expected, the conversion to $CaSO_4$ increased as the SO_2 concentration increased. A comparison between the test results in shown in figure 10.

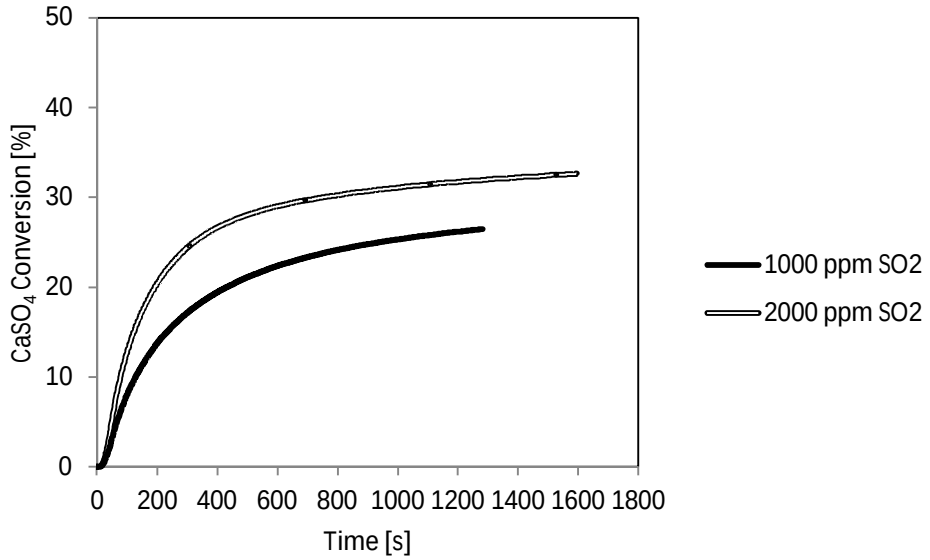

Figure 10 Effect of SO_2 concentration on sulfur capture based on laboratory measurements (air, T=850°C)

By observing the figure 10 it can be seen that the conversion rates are different right from the beginning of the reaction. With SO_2 concentration 1000 ppm, the final conversion to $CaSO_4$ was approximately 26 % whereas with SO_2 concentration 2000 ppm the conversion to $CaSO_4$ was about 32%.

The effects of smaller SO_2 concentration (1000 ppm SO_2) were also tested by means of modeling. The model based results are compared with the laboratory tests in figure 11.

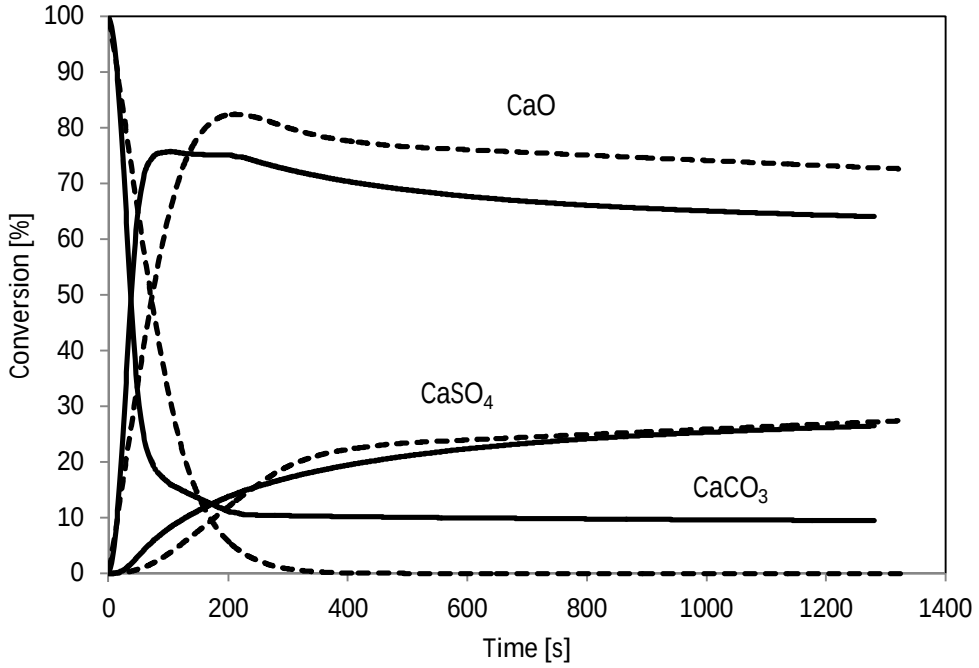

Figure 11 Simultaneous calcination–sulfation in air with 1000 vppm SO_2 at 850C. Measured values are marked with (—) and modeled values with (--).

In this case, the modeled and measured values do not give a very good response with each other. Despite this fact, it seems that the sulfation is first order with respect to SO_2. Theoretically the reaction order of SO_2 should be one, since the stoichiometric coefficient of SO_2 is one:

$$CaO(s) + SO_2(g) + \frac{1}{2}O_2(g) \longrightarrow CaSO_4(s). \qquad (50)$$

The modeled mass fraction of $CaSO_4$ inside the particle is shown in figure 12. As in the previous case, the sulfation seemed to obey core–shell structure, where the periphery of

the particle was highly sulfated (>50 %) while the inner parts remain less sulfated (~19 %).

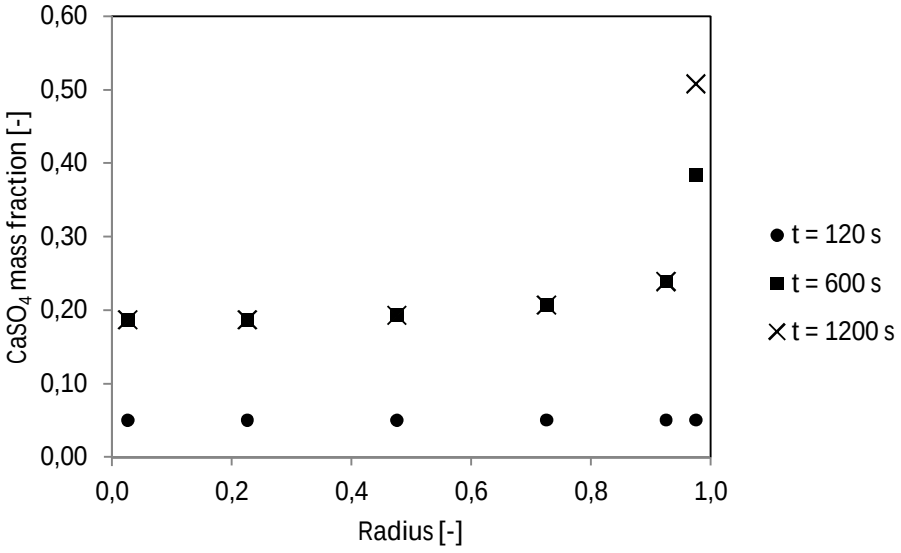

Figure 12 The modeled $CaSO_4$ mass fractions in the two outer elements as well as some inner parts the particle at different times at 1123 K (air with 1000 ppm SO_2).

The development of the effective diffusion coefficient inside the particle is shown in figure 13. In this case the diffusion coefficient through the product layer was higher since the outermost element remained less sulfated.

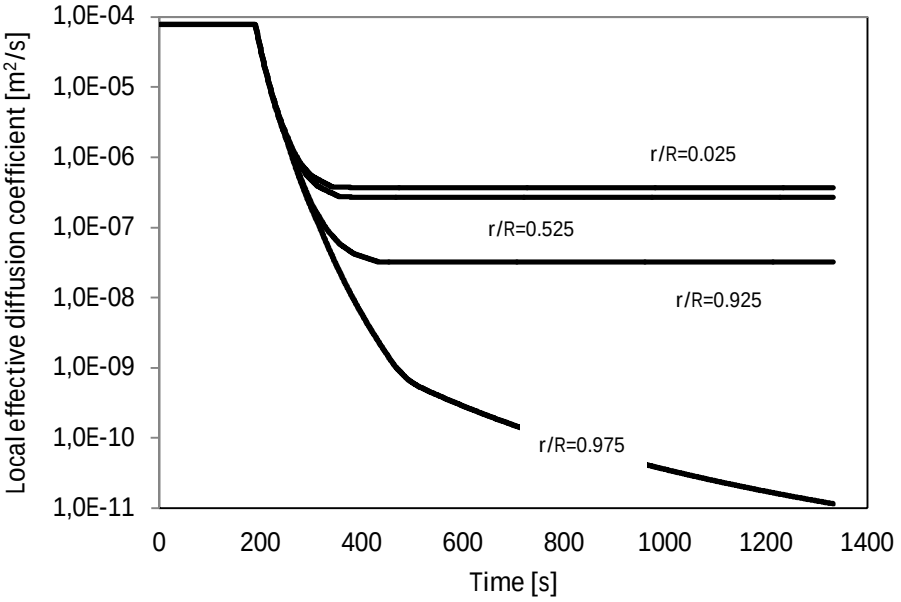

Figure 13 Development of local effective diffusion coefficient inside the particle at different times.

5.3 Effect of temperature

In one of the experiments the temperature was increased to 950 °C. It was noticed that the calcination was enhanced and the particle was completely calcined. With sulfation reaction, the change was much smaller, at 950 °C the final conversion to $CaSO_4$ was approximately 30%, whereas in the same conditions but at 850°C the conversion to $CaSO_4$ was about 32% (figure 14). It was concluded that in this case the optimal temperature level for sulfure capture was exceeded and consequently the sulfation was no more accelerated by increasing the temperature.

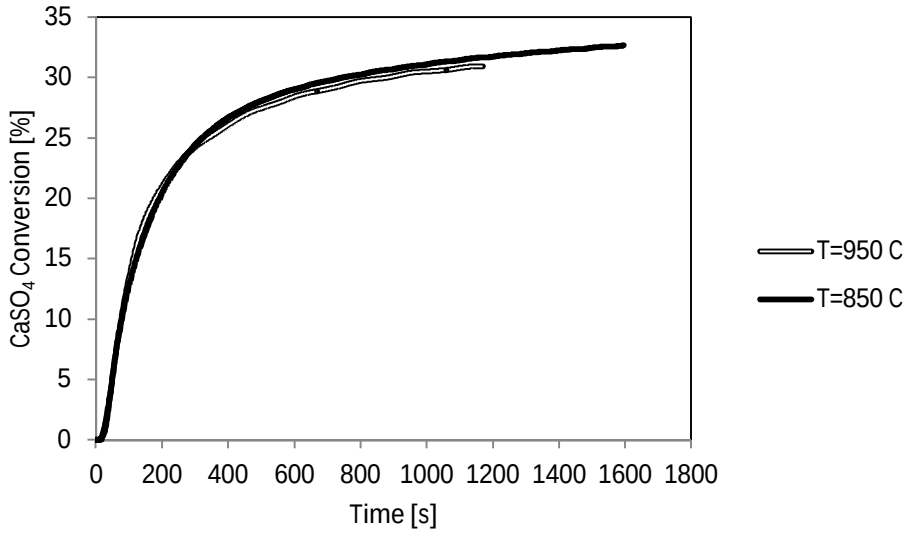

Figure 14 Effect on temperature on sulfure capture.

The conversion curves for the experimental and modeled values are shown in figure 15. It can be seen that in this case the modeled and the measured values give a good response with each other.

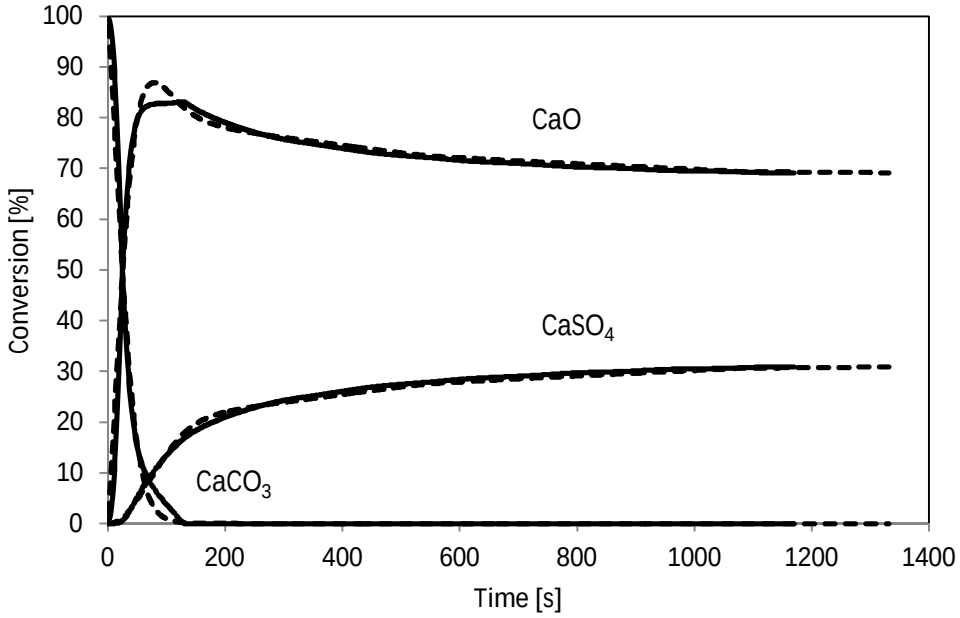

Figure 15 Conversion curves at 950°C. The laboratory tests are marked with (—) and modeled with (--).

The development of the effective diffusion coefficient inside the particle is shown in figure 16. The diffusion coefficient diminished drastically in the outermost periphery due to the formation of the sulfate layer.

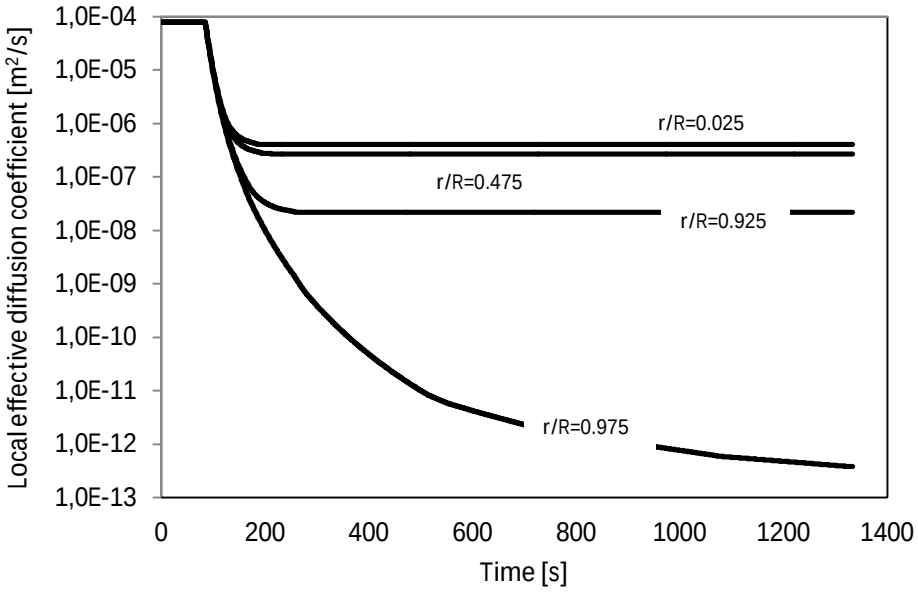

Figure 16 Development of local effective diffusion coefficient inside the particle at 950°C.

Figure 14 shows the development of Thiele modulus at 950 °C. In the beginning, the sulfure capture was only limited by reaction kinetics. After the initial period, the diffusion limitation increased and both reaction kinetics and diffusion had an effect.

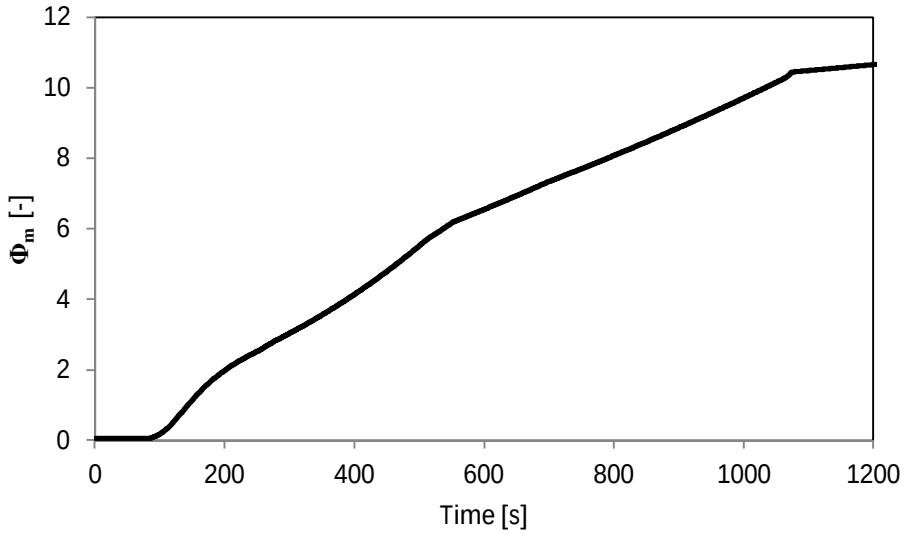

Figure 17 Development of Thiele parameter at 950 °C.

5.4 Effect of O_2 concentration

In the laboratory tests, three different oxygen concentrations were used, the test series are described in table 2.

Table 2. Test matrix, the temperature in all tests was 1123 K (850 °C).

Test number	**N_2 [%]**	**O_2 [%]**	**SO_2 [ppm]**
1	79	21	2000
2	90	10	2000
3	95	5	2000

The oxygen concentration was noticed to have an influence on both, calcination and sulfation reaction. Figure 18 shows the decomposition curves of $CaCO_3$ in different O_2 concentrations. By observing the graph it can be seen that the initial calcination rate is the same in each of the three tests but with final conversion some variation exits.

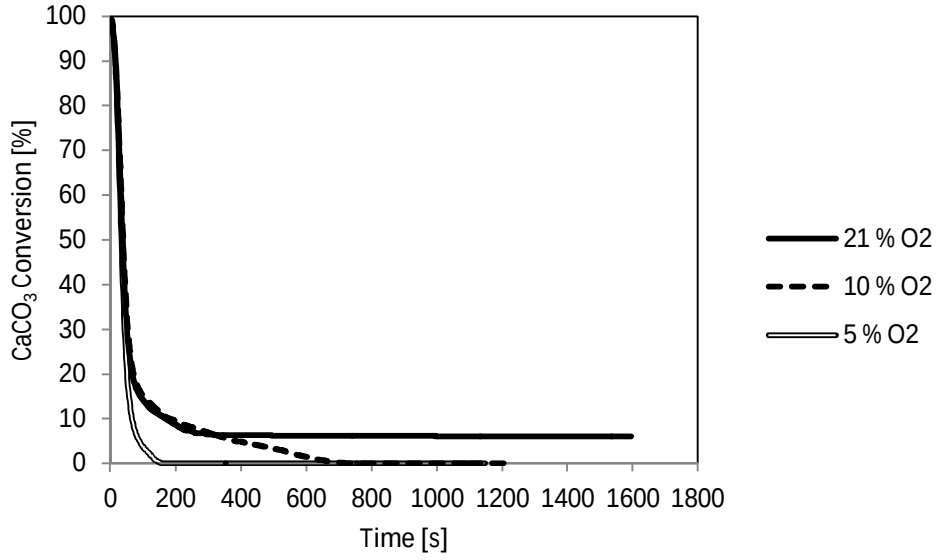

Figure 18 Effect of oxygen concentration on decomposition of $CaCO_3$.

In atmosphere containing 21 % O_2 approximately 6 % of the $CaCO_3$ didn't calcine but with oxygen concentrations 10 % and 5 % the particle was fully calcined. The decomposition of $CaCO_3$ after the initial stage was enhanced as the oxygen concentration was diminished.

Figure 19 shows the corresponding $CaSO_4$ conversion curves. With oxygen concentrations 21 % and 10 % there is not notable difference. In the experiment, where the concentration of O_2 was 5 %, a clear increase in the final $CaSO_4$ conversion was observed. In this case it could be simply thought that the conversion to $CaSO_4$ was higher because in these conditions the decomposition of $CaCO_3$ was faster after the initial stage than in the other cases. This enabled greater amount of fresh CaO available for sulfation. However, the systematic behavior especially in the $CaCO_3$ decomposition curves indicates that the oxygen concentration could possibly affect on the formation speed of $CaSO_4$ product layer. The non-porous product layer can prevent both the diffusion of SO_2 toward the particle interior and the movement of released CO_2 outward.

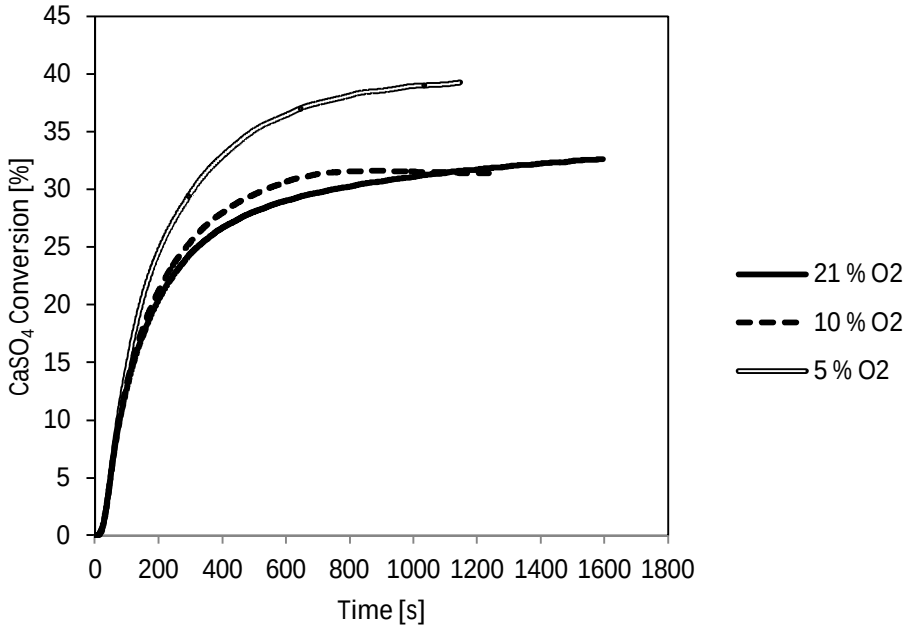

Figure 19 Effect of oxygen concentration on sulfur capture.

Dennis and Hayhurst (1990) studied the sulfation reaction in different oxygen concentrations and noticed that the oxygen concentration didn't affect on the initial sulfation rate but the ultimate conversion to $CaSO_4$ increased when the oxygen concentration was decreased. In the work of Dennis and Hayhurst (1990) it was discussed that the oxygen could affect to the crystal size or to the number of cracks in the $CaSO_4$ product layer. Dennis and Hayhurst (1990) also speculated that the sulfation might occur through intermediate stages. In their work the following reaction scheme was suggested:

$$CaO + SO_2 \rightarrow CaSO_3 \quad (51)$$

$$4CaSO_3 \rightarrow CaS + 3CaSO_4 \quad (52)$$

$$CaS + 2O_2 \rightarrow CaSO_4. \quad (53)$$

In this reaction series the calcium oxide reacts directly with SO_2 in and forms $CaSO_3$. The formed $CaSO_3$ is an unstable in temperatures above 970 K, and thus it decomposes fast to CaS and $CaSO_4$. Finally, the CaS is oxidized by O_2, so that the end product is

always $CaSO_4$. According to Dennis and Hayhurst (1990) also participation of ionic species $S_yO_x^{n-}$ is possible. In their study it was discussed that depending on the oxygen concentration, the structure of the product layer could be altering, relying on the rate of oxidation of sulphide (CaS) –or even sulphite ($CaSO_3$). In this case it can be noted that the molar volume of CaS (28.9 cm^3/gmol) is smaller than that of $CaSO_4$ (46.0 cm^3/gmol) and thus the diffusion resistance through the possible intermediate CaS would be smaller.

5.5 Sulfation characteristics based on SEM-EDS analysis

The physical characteristics of limestone such as, porosity, pore structure, crystal structure and sensitivity to fragmentation vary notably between different limestone types. These features may also affect significantly on the progress of the reactions. Structural and chemical analysis of the particles could be a useful tool to have information related to these properties and to increase the understanding of particle scale phenomena.

In this work the structure and characteristics of Endesa limestone were studied with aid of SEM-EDS analysis. Both uncalcined and sulfated limestone samples were analyzed and surface and cross-section analysis were done. Figure 20 shows the SEM images of the surfaces of uncalcined limestone. From this figure it can be seen that the particles have rather angular structure with small grains on the surface.

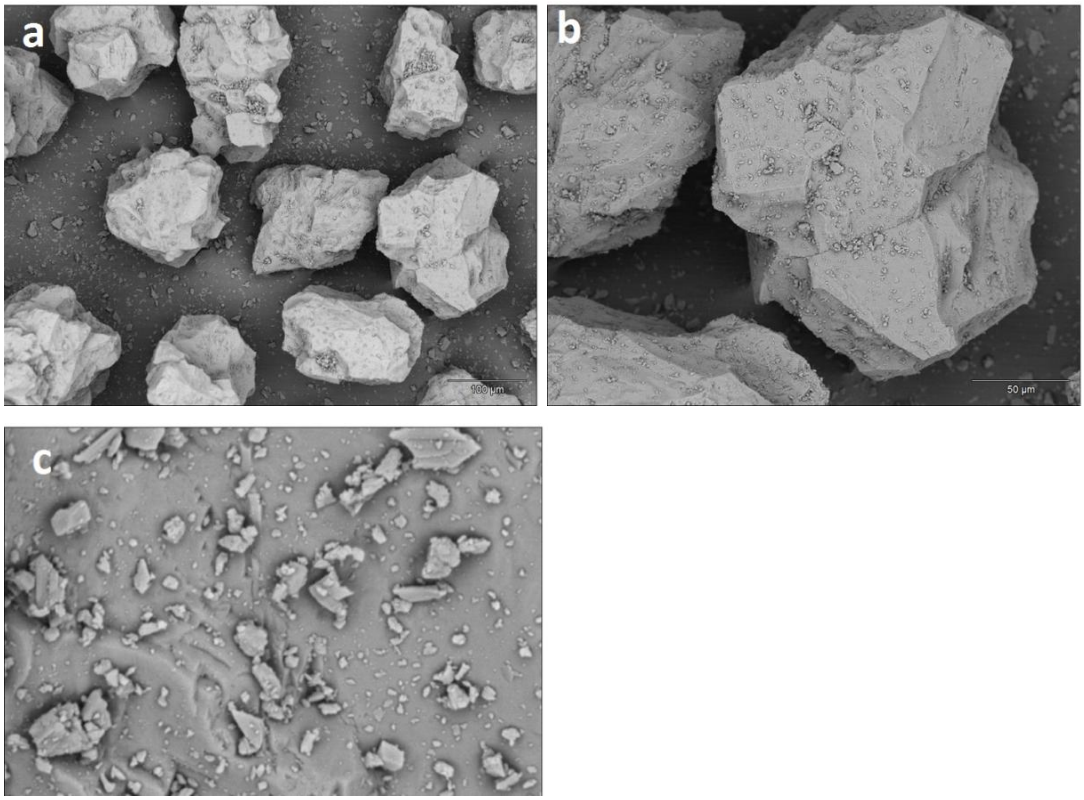

Figure 20 SEM images of uncalcined Endesa limestone. The pictures are taken with BEI -detector with accelerating voltage 10 kV. In figure a) limestone particles, magnification 200x, b) a single Endesa particle, magnification 500x, c) surface of a particle, magnification 5000x.

A sulfation experiment was carried out by using the Endesa limestone. The temperature in the experiment was 850°C and the gas atmosphere was containing 90% N_2, 10% O_2 and 2500 ppm SO_2. Figure 21 shows the SEM-EDS image of the sulfated Endesa limestone. The fragmentation of the sulfated particles was noticed to increase during the storing, although the particles were kept in a closed plastic container. This observation indicates that the SEM-EDS analysis of the samples should be done as soon as possible after they are removed from the boiler, or, the samples should be preserved in such a way that the possible interactions with the surrounding environment can be prevented.

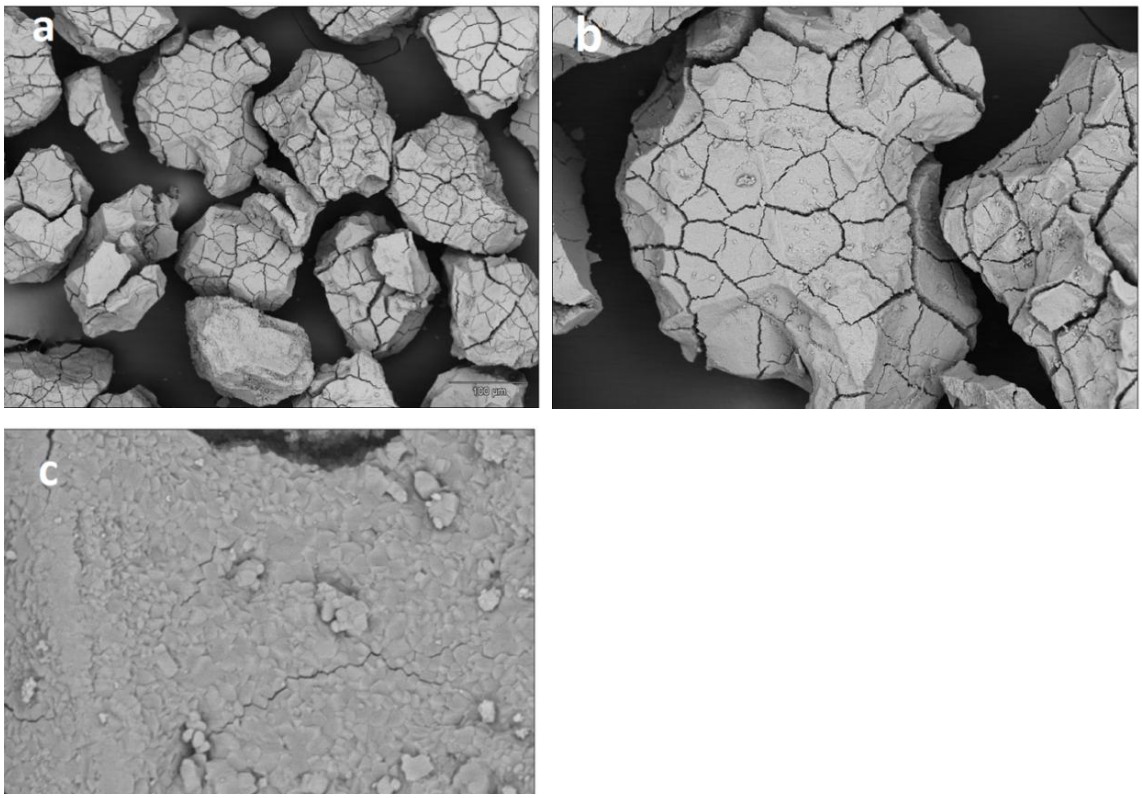

Figure 21 SEM –image of sulfated Endesa limestone. The pictures are taken with BEI –detector with accelerating voltage 10 kV. In figure a) sulfated limestone particles, magnification 200x, b) a single, sulfated Endesa particle, magnification 500x, c) surface of a particle, magnification 5000x.

The calcination–sulfation reactions changed especially the surface structure of the particle. The surface of the uncalcined Endesa limestone was rather smooth, with the small grains on top (figure 22a). After the sulfation, the surface was clustered (see figure 22b) which could possibly be a consequence of changes in the grain size due to calcination and sulfation reactions.

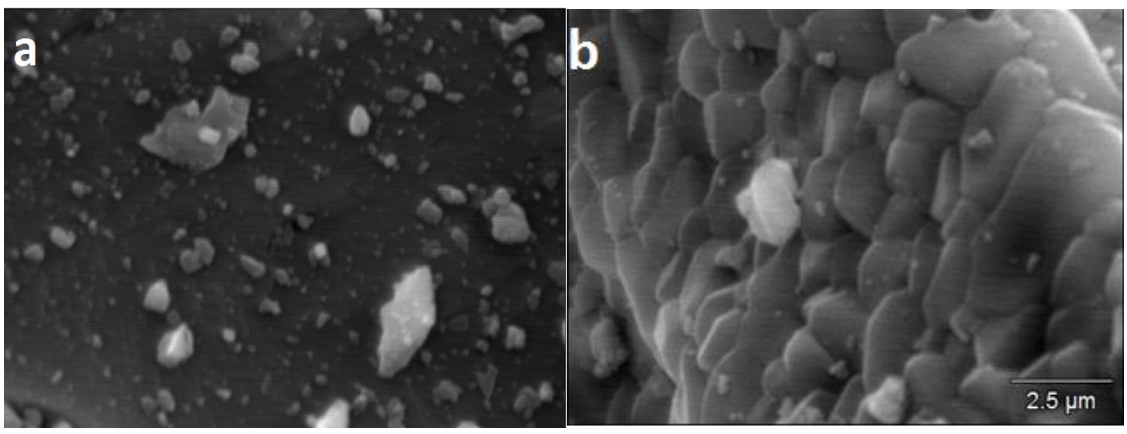

Figure 22 Surface of a) uncalcined Endesa limestone, b) sulfated Endesa limestone. Figures are taken with SEI-detector, with accelerating voltage 20 kV and magnification 10 000x.

In the work of Laursen *et al*. (2000) it was discussed that the sulfation pattern of the particles can be divided into three categories depending on the morphology and microstructure of the calcined limestone. According to Laursen *et al*. (2000) these categories are unreacted core, network and uniformly sulfated. The particles reacting according to unreacted core pattern have a highly sulfated outer periphery (70–95%) and unsulfated core (0–5%). Particles obeying network pattern are sulfated in the proximity of the fractures and around the periphery while being slightly or totally unsulfated in the areas separated by the fractures. The uniformly sulfated particles are described to have a relatively homogeneous sulfation degree (50–75%) in all parts of the particle.

In this study, it was noticed that the sulfation behavior of Endesa limestone seemed to obey the network structure. This can be observed from figures 23b and 23c, which show the distributions of elemental sulfur and elemental calcium in a cross-sectioned sample. Areas which are rich in sulfur appear dark in figure 23b. By observing the figure 23b, it can be seen that the particles are sulfated around the periphery and in the proximity of the fractures. The particle appearing with “uniform” sulfation degree (on the left in figure 23b) was not properly cross-sectioned and in this case the EDS –detector determined the sulfur distribution on the surface of the particle.

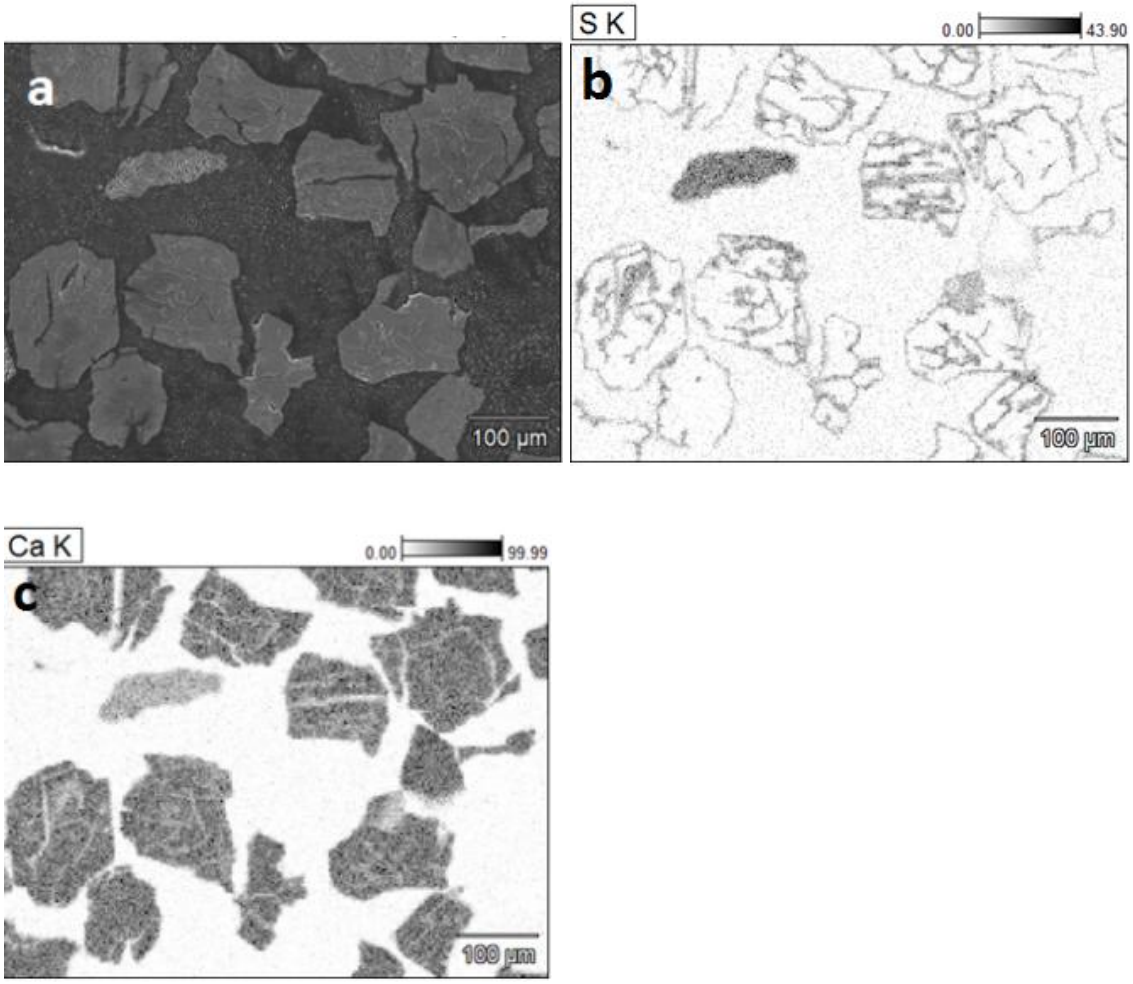

Figure 23 a) A cross-section of Endesa limestone particles. b) X-ray mapping of the sulfur distribution, areas which are rich in sulfur appear dark. c) X-ray mapping of the calcium distribution, areas which are rich in calcium appear dark. The accelerating voltage used was 20 kV.

To study the sulfation characteristics of Endesa limestone more detailed, two single particles were taken for further examination. Figure 24a shows a cross-section image of a single particle. The distribution of elemental sulfur and elemental calcium were determined and the results are shown in figures 24b and 24c. The mass fraction scale of the elements, which is mentioned above the figures 24b and 24c, should be considered as approximate. The $CaSO_4$ conversion degree was estimated in the specified areas, which are marked in figure 24d. The areas which are marked with numbers 1 and 2 in figure 24d, were free of sulfur. The areas marked with numbers 3 and 4 had an average $CaSO_4$ conversion degree of 52% and 35% respectively.

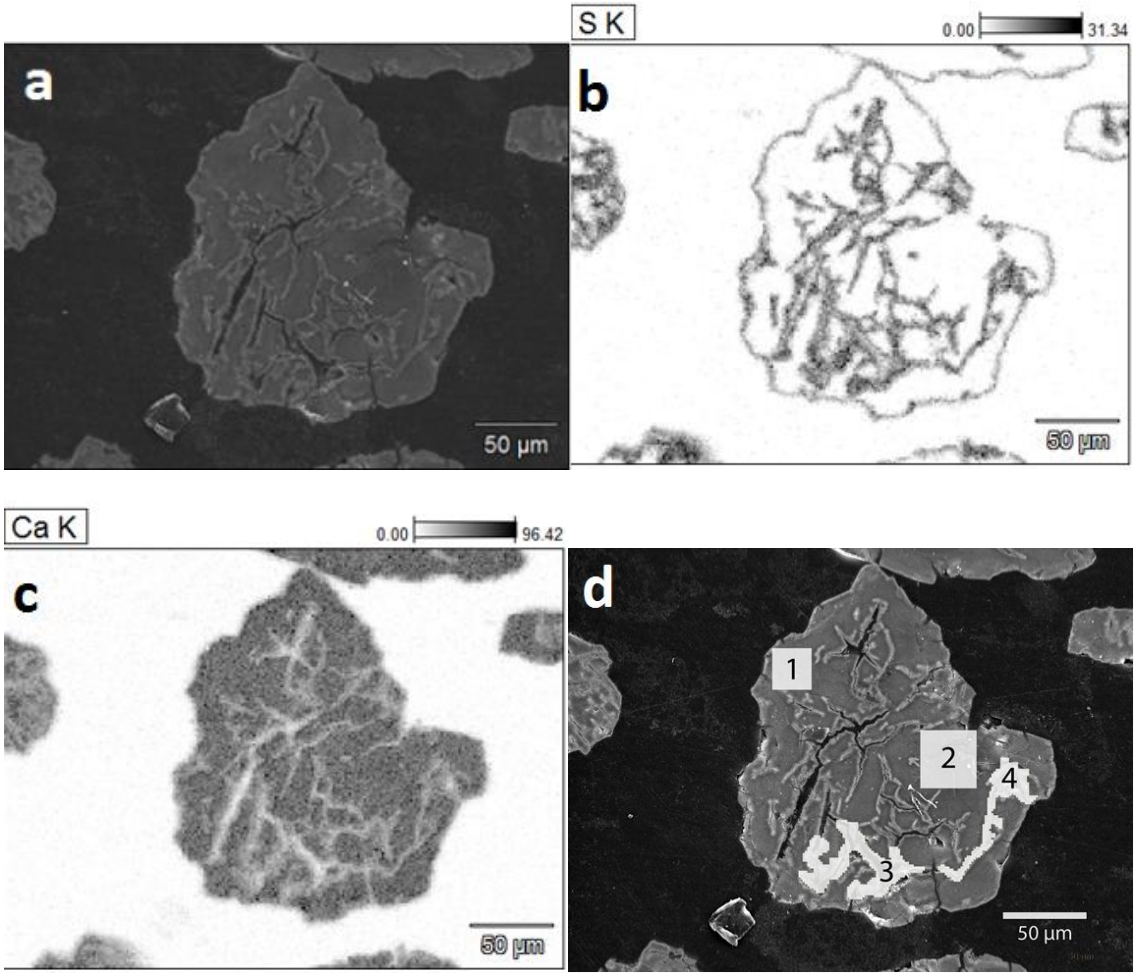

Figure 24 a) Cross-section of a sulfated Endesa limestone particle. b) X-ray mapping of the sulfur distribution in the particle c) X-ray mapping of the calcium distribution in the sample d) the $CaSO_4$ conversion degree was calculated on the specified areas marked in the figure. The accelerating voltage used was 20 kV.

Figure 25b shows a magnification of the sulfate rim on the particle periphery. From this figure it can be seen that the sulfate rim is rather narrow, the width is less than 5 µm. This observation indicates that with Endesa limestone, even a thin $CaSO_4$ product layer can prevent the progress of the reactions from the particle periphery towards the core.

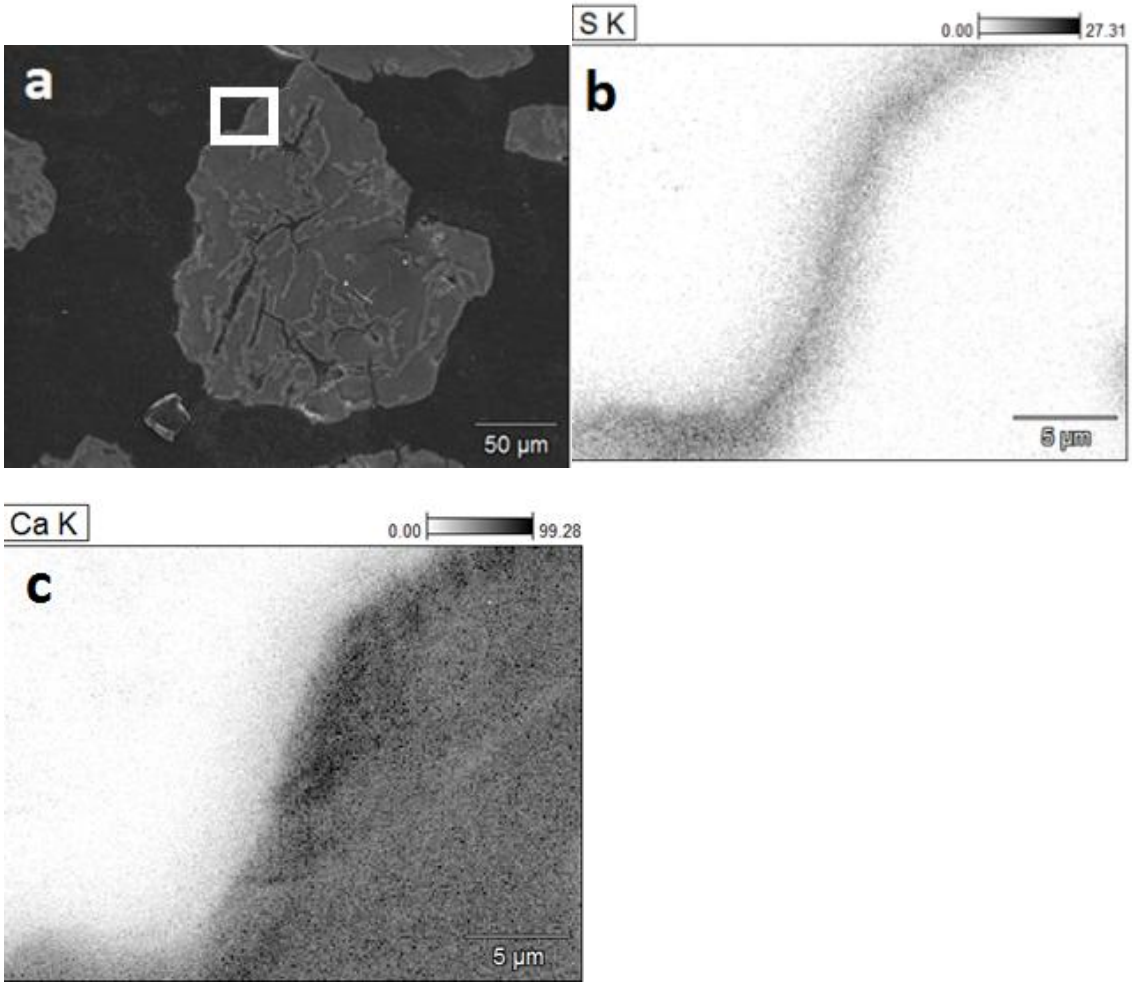

Figure 25. The X-ray mappings of b) sulfur and c) calcium distribution on the specified rectangular area marked in figure a).

Similar analyses were done also for another particle (figure 26). The distribution of elemental sulfur was determined for the whole particle (figure 26b) as well as for the specified rectangular area marked in figure 26a. The mass fraction scale for elemental sulfur (mentioned above the figures 26b and 26c) should be considered as approximate. By observing the figures 26b and 26c, it can be seen that the sulfated areas had an interconnected and tortuous structure. The conversion to $CaSO_4$ was determined in the specified areas marked in figure 26d. In the areas marked with numbers 1,2 and 3 the conversion to $CaSO_4$ was 0%. In the areas marked with 4 and 5 the conversion to $CaSO_4$ was approximately 56% and 59% correspondingly, revealing a rather similar $CaSO_4$ conversion degree as with the other particle described in figure 24.

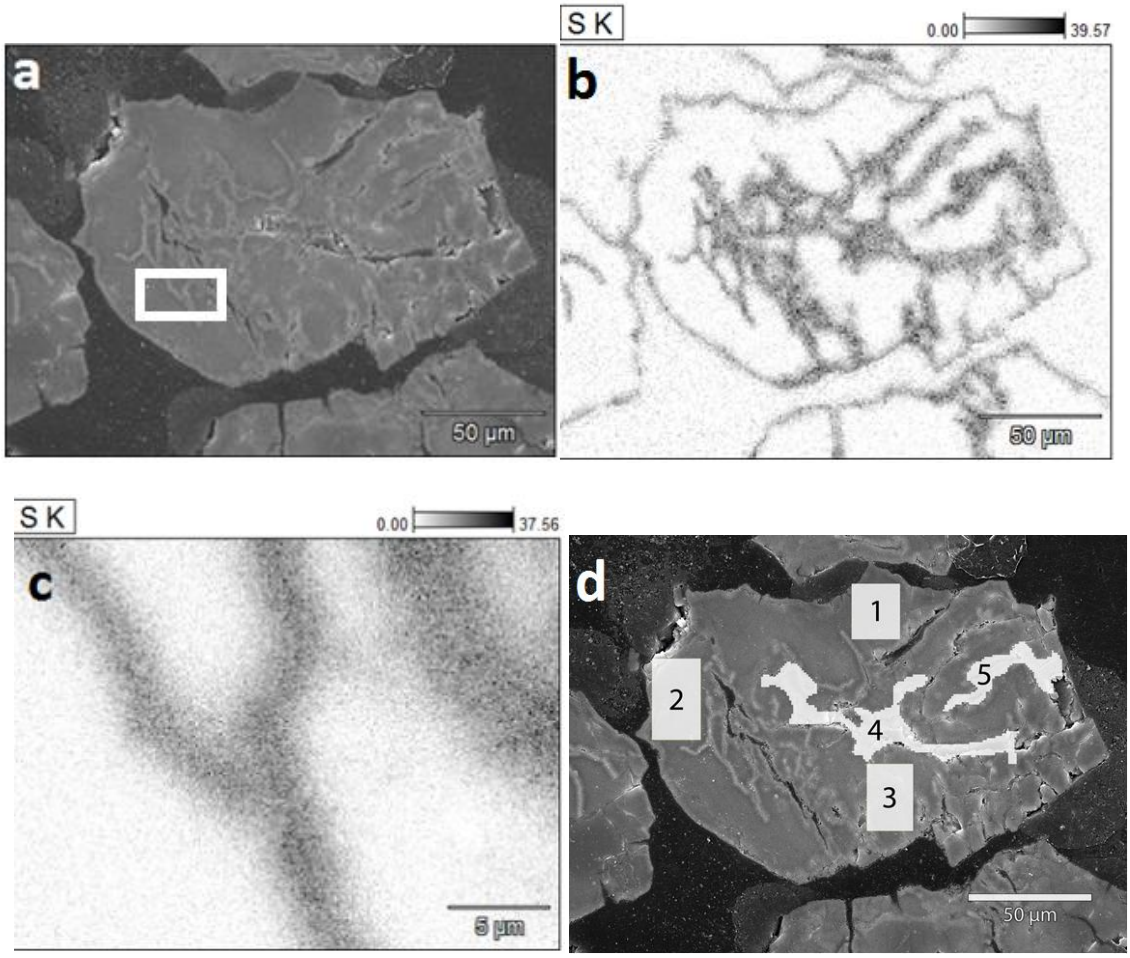

Figure 26 a) Cross-section of a sulfated Endesa limestone particle, b) X-ray mapping of the sulfur distribution in the particle, c) the sulfur distribution was determined on the rectangular area marked in the figure a, d) the $CaSO_4$ conversion degree was calculated on the specified areas marked in the figure. The accelerating voltage used was 20 kV.

It can be concluded that the fragmentation of the particles had a great influence on the sulfation of Endesa limestone in N_2/O_2 atmosphere. Without the fragmentation, the sulfur capture had probably been notably poorer, especially that the sulfate shell in the particle periphery seemed to be rather thin. From a modeling point of view, the network sulfation behavior is very difficult to predict and for example the traditional shrinking core model would not be a very good choice to describe the progress of the reactions for Endesa limestone. Possibly, a model which would consider the changes in the effective surface area due to chemical reactions and due to fragmentation could be a good modeling approach for Endesa limestone in the future studies.

6 CONCLUSIONS

Limestone reactions (calcination, sulfation, carbonation) in fluidized bed form a challenging area of study. The progress of the reactions can be significantly affected by the process conditions and by the type of limestone used in the boiler.

In new fluidized bed applications, such as oxy–fuel combustion and calcium–looping, the temperature levels and the composition of the flue gases differ from air-fired units and the conventional models cannot necessarily be used. The development of universally applicable models for large industrial scale requires profound understanding of particle scale phenomena. The study of particle scale level requires experimental test series in varying conditions, numerical modeling, chemical and structural analysis, and theoretical examination.

In this study, different methods (bench scale tests, numerical modeling and SEM-EDS analysis) were used to study the limestone reactions. It was observed that a higher sulfur dioxide concentration accelerated the sulfation reaction and based on the modeling, the sulfation seemed to be first order with respect to SO_2. By increasing the temperature from 850°C to 950°C calcination was accelerated but the sulfate conversion was no more improved. The apparent reaction order of oxygen seemed to become zero at high concentrations. The SEM-EDS analysis revealed that the sulfation of Endesa limestone in N_2/O_2 atmosphere was occurring in the periphery of the particle and in the proximity of the fractures.

BIBLIOGRAPHY

Abanades, J.C., Alvarez, D., Conversion limits in the reaction of CO_2 with lime, *Energy & Fuels* **17** (2003), 308-315.

Adanez, J., García-Labiano, F., Fierro, V., Modelling for the high-temperature sulphation of calcium-based sorbents with cylindrical and plate-like pore geometries, *Chemical Engineering Science* **55** (2000), 3665-3683.

Alvarez, D., Abanades, J.C. Determination of the critical product layer thickness in the reaction of CaO with CO_2, *Industrial & Engineering Chemistry Research* **44** (2005), 5608-5615.

Anthony E.J., Granatstein, D.L, Sulphation phenomena in fluidized bed combustion systems, *Progress in Energy and Combustion Science* **27** (2001), 215-236.

Anthony, E.J., Ca looping technology: current status, developments and future direction, Rewiew, *Greenhouse Gases: Science and Technology* **1** (2011), 36-47.

Baker, E.H., The calcium oxide-carbon dioxide system in the pressure range 1–300 atm, *Journal of the Chemical Society* **70** (1962), 464–470.

Berger, E., Effect of steam on the decomposition of limestone, *Industrial and Engineering Chemistry* **19** (1927), 594–596.

Blamey, J., Anthony, E.J., Wang, J., Fennel, P.S., The calcium looping cycle for large-scale CO_2 capture, *Progress in Energy and Combustion Science*, **36** (2010), 260-279.

Borgwardt, R. H. and Bruce, K. R., Reactivity of CaO with SO_2, *American institute of Chemical Engineers*, **32** (1986).

Charitos, A., Hawthorne, C., Bidwe, A. R., Sivalingam, S., Schuster, A., Spliethoff, H., Scheffknecht, G., Parametric investigation of the calcium looping process for CO_2 capture in a 10 kW_{th} dual fluidized bed, *International Journal of Greenhouse Gas Control* **4** (2010), 776-784.

Chen, C., Zhao, C., Mechanism of highly efficient in-furnace desulfurization by limestone under O_2/CO_2 coal combustion atmosphere, *Industrial & Engineering Chemistry Research* **45** (2006), 5078-5085.

Cussler, E.L., *Diffusion, Mass transfer in fluid systems* (Second edition) Cambridge University Press (1997).

Dam-Johansen, K., Hansen, P.F.B, Østergaard, K., High-temperature reaction between sulphur dioxide and limestone—III. A grain-micrograin model and its verification, *Chemical Engineering Science* **46** (1991), 847–853.

Dennis, J.S., Hayhurst, A.N. Mechanism of the sulphation of calcined limestone particles in combustion gases, *Chemical Engineering Science* **45** (1990), 1175-1187.

Duan, L., Zhao, C., Zhou, W., Qu, C., Chen, X., O2/CO2 coal combustion characteristics in a 50 kWth circulating fluidized bed, *International Journal of Greenhouse Gas Control* (2011).

García-Labiano, F., Abad, A., de Diego, L.F., Gayán, P., Adánez, J., Calcination of calcium-based sorbents at pressure in a broad range of CO_2 concentrations, *Chemical Engineering Science* **57** (2002), 2381-2393.

García-Labiano, F., Aránzazu, R., de Diego, L.F., de las Obras-Loscertales, Gayán, P., Abad, A., Adánez, J., Calcium-based sorbents behavior during sulphation at oxy-fuel fluidized bed combustion conditions, *Fuel* **90** (2011) 3100-3108.

Grasa, G., Murillo, R., Alonso, M., Abanades, C., Application of the random pore model to the carbonation cyclic reaction, *American Institute of Chemical Engineers*, **55** (2009), 1246–1255.

Hajaligol, M.R., Longwell, J.P., Sarofim, A.F., Analysis and Modeling of the direct sulfation of $CaCO_3$, *Industrial & Engineering Chemistry Research* **27**(1988), 2203–2210.

Hayhurst, A.N., Parmar, M.S., Measurement of the mass transfer coefficient and Sherwood number for carbon spheres burning in a bubbling fluidized bed, *Combustion and Flame* **130** (2002), 361–375.

Hu, G., Dam-Johansen, K., Wedel, S., Hansen, J. P., Review of the direct sulfation of limestone, *Progress in Energy and Combustion Science* **32** (2006), 386–407.

Hu, G., Dam-Johansen, K., Wedel, S., Kinetics of the direct sulfation of limestone at the initial stage of crystal growth of the solid product, *American Institute of Chemical Engineers*, **57** (2011), 1607–1616.

Hu, G., Dam-Johansen, Wedel, S., Hansen, J. P., Direct sulfation of limestone, *American Institute of Chemical Engineers* **53** (2007), 948–960.

Hu, N., Scaroni, A.W., Calcination of pulverized limestone particles under furnace injection conditions, *Fuel* **75** (1996), 177–186.

Khinast, J., Krammer, G.F., Brunner, Ch. Staudinger, G., Decomposition of limestone: the influence of CO_2 and particle size on the reaction rate, *Chemical engineering science* No4, **51** (1996), 623–634.

Laursen, K., Duo, W., Grace, J.R., Lim, J., Sulfation and reactivation characteristics of nine limestones, *Fuel* **79** (2000) 153–163.

Lee, D.K. An apparent kinetic model for the carbonation of calcium oxide by carbon dioxide, *Chemical Engineering Journal*, **100** (2004), 71–77.

Levenspiel, O., *Chemical reaction engineering*, John Wiley & Sons (1999), Third edition

Levitz, P. Knudsen diffusion and excitation transfer in random porous media, *The Journal of Physical Chemistry* **97** (1993), 3813–3818.

Liu, H., Katagiri, S., Kaneko, K., Okazaki, K., Sulfation behavior of limestone under high CO_2 concentration in O_2/CO_2 coal combustion, *Fuel* **79** (2000), 945–953.

Lu, D., Hughes, R.W. Anthony, E. J., Ca-based sorbent looping combustion for CO_2 capture in pilot-scale dual fluidized beds, *Fuel Processing Technology* **89** (2008) 1386–1395.

Manovic, V. and Anthony, E., Sulfation Performance of CaO –Based Pellets Supported by Calcium Aluminate Cements Designed for High-Temperature CO_2 Caprture, *Energy & Fuels* **24** (2010), 1414–1420.

Manovic, V., Anthony, E.J., Carbonation of CaO –based sorbents enhanced by steam addition, *Industrial & Engineering Chemistry Research* **49** (2010), 9105-9110.

Mattisson, T., Lyngfelt, A., A sulfur capture model for circulating fluidized-bed boilers, *Chemical Engineering Science* **53** (1998), 1163–1173, I.

Mattisson, T., Lyngfelt, A., Reaction between sulfur dioxide and limestone under periodically changing oxidizing and reducing conditions–effect of cycle time, *Energy & Fuels* **12** (1998), 905–912. II

Mess, D., Sarofim, A.F., Longwell, J.P., Product layer diffusion during the reaction of calcium oxide with carbon dioxide, Energy & Fuels **13** (1999), 999–1005

Milne, C.R., Silcox, G. D., Pershing, D.W., Kirchgessner, D.A., Calcination and sintering models for application to high-temperature short time sulfation of calcium-based sorbents, *Industrial & Engineering Chemistry Research*, **29** (1990), 139–149.

Myöhänen, K., Hyppänen, T., Pikkarainen, T., Eriksson, T., Hotta, A., Near zero CO_2 emissions in coal firing with oxy-fuel circulating fluidized bed boiler, *Chemical Engineering & Technology* **32** (2009), 355–363.

Rao, R., Kinetics of Calcium Carbonate Decomposition, *Chemical Engineering & Technology*, **19** (1996), 373-377.

Ray, H.S., The kinetic compensation effect in the decomposition of calcium carbonate, *Journal of Thermal Analysis* **24** (1982), 35–41.

Saastamoinen, J., Pikkarainen, T., Tourunen, A., Räsänen, M., Jäntti, T., Model of fragmentation of limestone particles during thermal shock and calcinations in fluidized beds, Powder Technology **187** (2008), 244–251.

Sánchez-Biezma, A., Ballesteros, J.C., Diaz, L., de Zárraga, E. Álvarez, F.J., López, J., Arias, B., Graza, G., Abanades, J.C., Postcombustion CO_2 capture with CaO. Status of the technology and next steps towards large scale demonstration, *Energy Procedia* **4** (2011), 852–859.

Scala, F., Cammarota, R.C., Salatino, P., Comminution of limestone during batch fluidized-bed calcination and sulfation, *American Institute of Chemical Engineers* **43** (1997), 363–373.

Silcox, G.D., Kramlich, J.C., Pershing, D.W., A mathematical model for the flash calcination of dispersed $CaCO_3$ and $Ca(OH)_2$ particles, *Industrial & Engineering Chemistry Research* **28** (1989), 155–160.

Snow, M. J.H., Longwell, J.P., Sarofim, A., Direct sulfation of calcium carbonate, *Industrial & Egineering Chemistry Research*, **27** (1988), 268–273.

Stanmore, B.R., Gilot, P., Review–calcination and carbonation of limestone during thermal cycling for CO_2 sequestration, *Fuel Processing Technology* **86** (2005), 1707-1743.

Stewardt, M.C., Manovic, V., Anthony, E.J., Macchi, A., Enhancement of indirect sulphation of limestone by steam addition, *Environmental Science and Technology* **44** (2010), 9781–8786.

Sun, P., Grace, J.R., Jim Lim, C., Anthony, E.J. Determination of intrinsic rate constant of the CaO –CO_2 reaction, *Chemical Engineering Science* **63** (2008) 47–56, I

Sun, P., Grace, J.R., Lim, C.J., Anthony, E.J., A discrete-pore-size-distribution-based gas-solid model and its application to the CaO + CO_2 reaction, *Chemical Engineering Science* 63 (2008) 57–70, II

Takkinen, S., Hyppänen, T., Saastamoinen, J., Pikkarainen, T., Experimental and modeling study of sulfur capture by limestone in selected conditions of air-fired and oxy-fuel circulating fluidized-bed boilers, *Energy & Fuels* **25** (2011), 2968–2979.

Wang, C., Jia, L., Tan, Y., Anthony, E.J., Influence of Water Vapor on the direct sulfation of limestone under simulated oxy-fuel fluidized bed combustion (FBC) conditions, *Energy Fuels*, **25** (2011), 617–623.

Wang, C., Jia, L., Tan, Y., Anthony, E.J., The effect of water on the sulphation of limestone, *Fuel* **89** (2010), 2628–2632.

Wang, Y., Lin, S, Suzuki, Yoshizo Limestone Calcination with CO_2 Capture (II): Decomposition in CO_2/Steam and CO_2/N_2 Atmospheres , *Energy & Fuels* **22** (2008), 2326–2331.

Wang, Y., Lin, S., Suzuki, Y., Experimental study on CO_2 capture conditions of fluidized bed limestone decomposition reactor, *Fuel Processing Technology* **91** (2010), 958–963.

Zhao, C.S, Duan, L.B., Chen, X.P., Liang, C., Latest evolution of oxy-fuel combustion technology in circulating fluidized bed, Proceedings of the 20th International Conference on Fluidized Bed Combustion, 2010, 49–58.